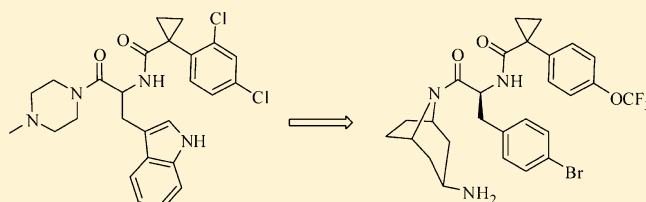


Discovery and Characterization of an Inhibitor of Glucosylceramide Synthase

Steven Richards,^{*,†} Christopher J. Larson,[†] Elena S. Koltun, Art Hanel, Vicky Chan, Jason Nachtigall, Amanda Harrison, Naing Aay, Hongwang Du, Arlyn Arcalas, Adam Galan, Jeff Zhang, Wentao Zhang, Kwang-Ai Won, Danny Tam, Fawn Qian, Tao Wang, Patricia Finn, Kathy Ogilvie, Jon Rosen, Ron Aoyama, Artur Plonowski, Belinda Cancilla, Frauke Bentzien, Michael Yakes, Raju Mohan, Peter Lamb, John Nuss, and Patrick Kearney

Exelixis, Inc., 210 E. Grand Avenue, South San Francisco, California 94080, United States

ABSTRACT: Targeting glycosphingolipid synthesis has emerged as a novel approach for treating metabolic diseases. **32** (EXEL-0346) represents a new class of glucosylceramide synthase (GCS) inhibitors. This report details the elaboration of hit **8** with the goal of achieving and maintaining maximum GCS inhibition in vivo. **32** inhibited GCS with an IC_{50} of 2 nM and achieved maximum hepatic GCS inhibition after four or five daily doses in rodents. Robust improvements in glucose tolerance in DIO mice and ZDF rats were observed after 2 weeks of q.d. dosing. Four weeks of dosing resulted in decreased plasma triglycerides and reduced hepatic fat deposition. Thus, **32** provides insight into the amount of metabolic regulation that can be restored following achievement of maximal target knockdown.



INTRODUCTION

Type 2 diabetes is a condition that affects millions in the United States. The prevalence of the disease has increased as the “Western” culture of calorie rich diet and sedentary lifestyle has spread throughout the world. In 2007, diabetes was the seventh leading cause of death in the U.S. and cost well over \$100 billion to treat.¹ Current pharmaceutical interventions work, alone or in combination, via a variety of mechanisms to lower hepatic glucose output, inhibit glucose uptake, slow gastric emptying, increase insulin sensitivity, and stimulate insulin secretion.² Despite these advances, there remains significant interest in new molecular targets whose modulation could regulate glucose and lipid metabolism.

One such target is glucosylceramide synthase (GCS). GCS regulates the production of glycosphingolipid conjugates called gangliosides (such as **3** (GM3)) via glucosyl transfer to **1** (ceramide, Figure 1). Improper regulation of the direct product of this reaction, **2** (glucosylceramide), results in a rare metabolic disorder known as Gaucher disease. This lysosomal storage disease arises from a genetic lack of the enzyme glucosylcerebrosidase, which degrades glucosylceramide. The clinical manifestations of this disorder include thrombocytopenia, splenomegaly, increased liver size, and debilitating bone pain.³ In this context, small molecule inhibition of GCS has proven effective. Iminosugar **4** (migustat), shown in Figure 2, is used as substrate reduction therapy (SRT) for Gaucher patients in lieu of enzyme replacement therapy (ERT).⁴ Ceramide analogue **5** (Genz-112638) is in clinical development to treat type 1 Gaucher disease.⁵

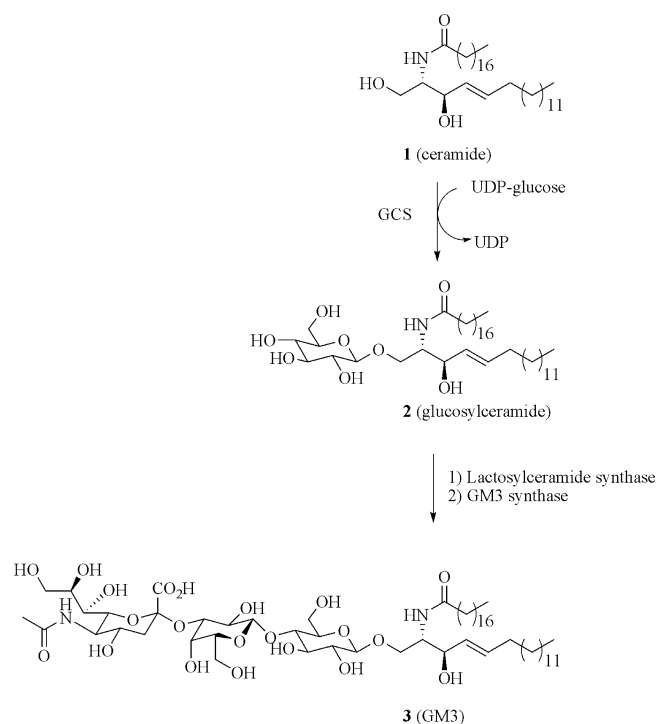


Figure 1. GCS mediated glycosphingolipid synthesis.

Received: January 27, 2012

Published: April 12, 2012

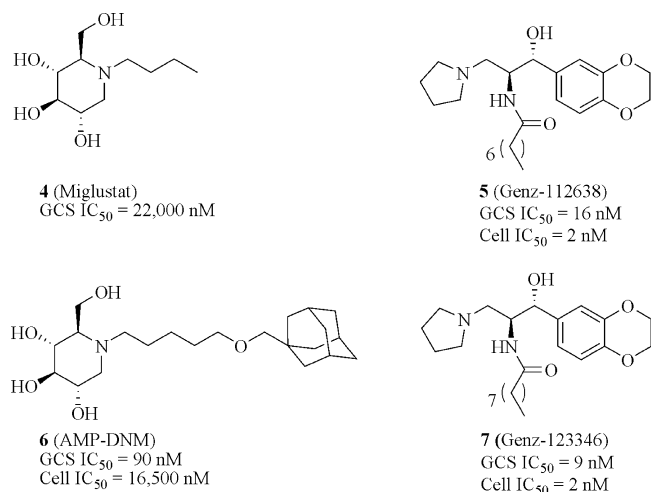


Figure 2. Representative GCS inhibitors.⁸

In the past decade, excess ganglioside GM3 has been shown to disrupt insulin receptor function. Mice lacking GM3 exhibited increased glucose tolerance and improved insulin receptor (IR) phosphorylation.⁶ The mechanistic hypothesis for this dysregulation is that excess GM3 in the cell membrane forms lipid rafts that disrupt the membrane environment around the insulin receptor. Because of this perturbation, the insulin receptor does not signal properly resulting in insulin resistance.⁷ In this context, small molecule GCS inhibition has also been beneficial.

Iminosugar **6** (AMP-DNM) both decreased cell surface GM3 and increased insulin stimulated IR phosphorylation in 3T3L1 adipocytes. In vivo effects include improved oral glucose tolerance and decreased glycated hemoglobin (% HbA1c).⁹ The effects were observed after dosing for 10 weeks at 25 mpk in Zucker diabetic fatty (ZDF) rats and correlated with decreased hepatic glucosylceramide levels. Additional metabolic improvements were measured after dosing **6** for 5 weeks at 100 mpk in another diabetic rodent model, the *ob/ob* mouse. Increased insulin receptor activation, represented by increased hepatic pAkt and pmTOR, and normalization of the expression of several proteins related to hepatic lipid metabolism and gluconeogenesis were observed. Additionally, hepatic fat depots were decreased after treatment with **6**.¹⁰ Iminosugar **6** is also a potent inhibitor of intestinal glucosidases which contributes to the observed antidiabetic efficacy.¹¹

Ceramide analogue **7** (Genz-123346) has also demonstrated metabolic improvements after chronic administration.¹² In ZDF rats, a striking decrease in HbA1c was observed after 6 weeks of dosing at 75 mpk. Decreased hepatic glucosylceramide was measured after 10 weeks of dosing **7** at 85 mpk. In diet induced obese (DIO) mice, near normalization of glucose excursion during an oral glucose challenge was achieved after dosing **7** for 10 weeks at 125 mpk. Again, this was accompanied by a marked improvement in HbA1c. In both rodent models, efficacy was driven by restoration of insulin receptor function. Treatment with **7** (125 mpk for 12 or 20 weeks) also reversed hepatic steatosis in DIO mice.¹³

In recent studies supported by Genzyme, treatment with ceramide analogue **5** modulated hepatic ceramide, glucosylceramide, and GM3 in lean mice. These effects were observed after dosing these animals for 22 weeks at 120 mpk. In DIO mice, **5** lowered HbA1c after 12 weeks of dosing at either 75 or 125 mpk.

Glucose tolerance, as demonstrated by an IGTT, was improved after 10 weeks of dosing at 125 mpk. These animals had lower whole body fat mass, decreased liver triglycerides, and decreased liver fat deposition.¹⁴

Inspired by these reports, we structured our research program to provide further support for the clinical management of type 2 diabetes via GCS inhibition. One aspect of our approach was an interest in leveraging our screening platform to identify novel scaffold classes. Early work in this area has been previously reported.¹⁵ The other pillar of our approach was an interest in achieving sustained GCS inhibition in vivo in an attempt to determine how quickly antidiabetic efficacy would result. This report details the achievement of the second goal, the discovery and characterization of **32** (EXEL-0346), a potent, efficacious GCS inhibitor.¹⁶

RESULTS AND DISCUSSION

Our HTS campaign surveyed our collection of over 4 million compounds. One of the hits was the racemic tryptophan based dipeptide (**8**) shown in Figure 3. When both enantiomers of

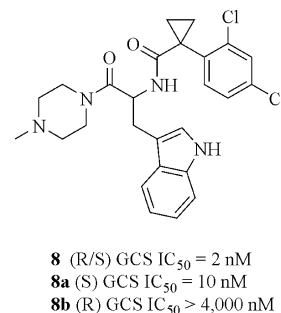
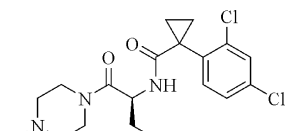


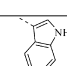
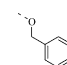
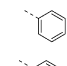
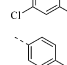
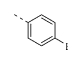
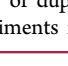
Figure 3. HTS hit.

the HTS hit (**8**) were synthesized, the *S* enantiomer (**8a**, derived from *L*-tryptophan) was found to be responsible for the observed activity against GCS. Epimeric **8b** was inactive. This strong correlation between GCS activity and amino acid stereochemistry was found to be general after several analogous enantiomer pairs were synthesized (data not shown). Thus, we proceeded with SAR development with analogues derived from *L*-amino acids.

Further characterization of **8a** revealed that it was also active in our GM1 depletion cell assay. ADME profiling further revealed instability to mouse microsomal oxidation and a modest CYP3A4 liability. We were first interested in understanding the impact of tryptophan replacement on potency and ADME properties. A summary of these efforts is presented in Table 1. The results of a broad survey of amino acids is not presented here, as most were not tolerated. However, benzylserine analogue **11**, while less potent than **8a**, was tolerated. Additionally, it showed that the ADME profile could be influenced by the amino acid. A slight improvement in microsomal stability and increased affinity for CYP3A4 were the result. Phenylalanine derivative **17** was also tolerated but was 15-fold less potent than hit **8a** with no ADME benefit. Fortunately, modification of the phenylalanine restored the biochemical and cell potency to this subseries, as evidenced by compounds **18–20**. Unfortunately, compounds **18–20** were no more stable in mouse microsomes than **8a** and were all about 10-fold more potent inhibitors of CYP3A4. Thus, our efforts to try to modify the amino acid moiety were successful only in part.

Table 1. Amino Acid Derivatives



Compound	R	GCS IC ₅₀ (nM) ^a	Cell IC ₅₀ (nM) ^{b,c}	MLMO (% conversion)	CYP3A4 IC ₅₀ (nM)
8a		10	6	90	10,000
11		90	330	50	2,200
17		160	n.d.	80	1,360
18		12	4	80	1,030
19		10	3	73	760
20		7	14	90	480

^aAverage value of duplicate experiments reported. ^bAverage value of triplicate experiments reported. ^cn.d. = value not determined.

With compounds in hand that represented two subseries, an effort was made to differentiate them in vivo. As shown in Table 2, 100 mpk doses of hit **8a** and **18** were given orally to

Table 2. Mouse Plasma Exposure of Lead Compounds **8a** and **18**

compd	1 h [plasma] (μM) ^a	4 h [plasma] (μM) ^a
8a	0.9 \pm 0.5	0.7 \pm 0.3
18	4.2 \pm 1.6	5.8 \pm 1.7

^aFemale nude mouse ($n = 3$), 100 mpk, po. Values reported are the mean \pm SD.

mice, and compound levels were measured 1 and 4 h after dosing. In these experiments, **18** had higher plasma levels at both measured time points than **8a**. Our shift in research focus to phenylalanine analogues was driven largely by the results of this screening PK experiment. Our goal became to address the ADME liabilities of **18** with an analogue that had comparable or improved potency and exposure.

With the amino acid core in place, we turned our attention to the other poles of the scaffold. A summary of these efforts is presented in Table 3. A metabolite identification experiment performed on **18** determined that the *N*-methylpiperazine moiety was the primary site of oxidative metabolism (data not shown). Piperazine **21**, one of the putative metabolites, was 10-fold less potent than **18**. What was of more concern was the potent CYP3A4 inhibition exhibited by this compound (CYP3A4 IC₅₀ < 200 nM). When the methyl group was transposed from the N4 to the C3 position on the piperazine ring, the resulting diastereomers **22** and **23** were also tolerated. Compound **22** (GCS IC₅₀ = 20 nM) was equipotent to **18**, and **23** (GCS IC₅₀ = 190 nM) was equipotent to **21**. Unfortunately, both compounds had the same severe CYP3A4 liability. Given the potent CYP3A4 inhibition for this set of compounds, it was difficult to interpret the increased metabolic stability they exhibited relative to **18**. Taken together, these data suggested that the piperazine moiety had to be replaced rather than modified.

To that end, compound **24** was prepared. This “ring opened” piperazine analogue was biochemically about 5-fold more potent than **18**. Cellular potency was about 30 fold lower (GCS cell IC₅₀ = 120 nM). The CYP profile and susceptibility to microsomal oxidation were not improved. The bromophenylalanine analogue **25** (GCS IC₅₀ = 4 nM) was equipotent to **24** biochemically. Fortunately, the modification of the phenylalanine ring provided a 7-fold improvement in cellular potency relative to **24**. Compound **25** also showed about a 5-fold decrease in CYP3A4 potency relative to **18**. However, microsomal stability was not improved. From this set of compounds, we learned that the piperazine could indeed be replaced and that modifications to the amino acid core could have a beneficial impact on cell potency and CYP profile.

We also confirmed that a basic amine was necessary for potency in this series. A representative example of this is compound **26**. With a hydroxyl group, **26** was tolerated (GCS IC₅₀ = 260 nM) but was 100-fold less potent than 4-aminopiperidine **27** (GCS IC₅₀ = 3 nM). Additionally, compound **27** had a better CYP profile. Metabolic stability of the two compounds was similar.

Compound **27** also taught us that a 1,5-diamino substitution pattern was well tolerated. This observation was confirmed by the synthesis of 3-aminopiperidine **28**. While the metabolic stability of this compound was quite good, it was a very potent CYP inhibitor (CYP3A4 IC₅₀ = 420 nM). Further constraint of the 1,5-diamino motif into an aminotropane resulted in **29**. Compound **29** (GCS IC₅₀ = 4 nM) was 4-fold more potent than **28** and especially potent in cells (GCS cell IC₅₀ = 2 nM). However, like **28**, **29** was a potent CYP3A4 inhibitor. An attempt to modify the amino acid portion to improve the CYP3A4 profile, as we had with **25**, was not successful. Compound **30** had a biochemical and ADME profile identical to that of **29** while losing 20-fold cellular potency. Fortunately, modification of the cyclopropylaryl moiety provided a way forward. In general, modification of this region of the scaffold was very poorly tolerated. One of the few reasonable substituents was the 4-trifluoromethoxy group. When incorporated, this group helped compound **31** (GCS IC₅₀ = 3 nM) maintain the biochemical potency observed in compounds **29** and **30**. Cell activity of **31** (GCS cell IC₅₀ = 8 nM), while 4-fold worse than **29**, was still within a desirable range. The most significant profile improvement was the 5-fold decrease in CYP3A4 potency exhibited by **31** (CYP3A4 IC₅₀ = 2.4 μM). Combining the bromophenylalanine substituent with the 4-trifluoromethoxyphenylcyclopropamide led to compound **32**. Again, biochemical and cell potency were comparable to **31** as was the ADME profile. Since it possessed a balanced in vitro profile, **32** was advanced into PK to compare with compound **18**. The aim was to help us understand to what extent in vitro ADME improvements could help us achieve the desired in vivo exposure profile.

Our goal was to discover a GCS inhibitor that could achieve sustained target knockdown between doses. Theoretically, the resulting cell surface ganglioside depletion would restore insulin receptor function and lead to improved glucose control. Table 4 is a summary of rodent PK data obtained for **32**. In the mouse screening PK experiment, a 10 mpk dose of **32** resulted in 24 h exposure in liver, muscle, and fat well in excess of the cellular IC₅₀ of the compound. In order to achieve comparable 5.9 μM liver exposure of **18** at 24 h, a 30–75 mpk dose was required. Additionally, **32** plasma exposure was relatively low. This was thought to be an advantage for the compound, as the benefit of GCS inhibition would be in tissues

Table 3. Identification of 32

Compound	R ₁	R ₂	R ₃	R ₄	R ₅	GCS IC ₅₀ (nM) ^a	Cell IC ₅₀ (nM) ^{b,c}	MLMO (% conversion) ^c	CYP3A4 IC ₅₀ (nM) ^c
21		Cl	Cl	Cl	Cl	150	n.d.	10	< 200
22		Cl	Cl	Cl	Cl	20	n.d.	30	450
23		Cl	Cl	Cl	Cl	190	n.d.	40	400
24		Cl	Cl	Cl	Cl	2	120	70	1,530
25		H	Br	Cl	Cl	4	10	90	7,800
26		H	Br	Cl	Cl	260	n.d.	30	1,300
27		H	Br	Cl	Cl	3	n.d.	50	8,000
28		Cl	Cl	Cl	Cl	16	n.d.	10	420
29		Cl	Cl	Cl	Cl	4	2	20	430
30		H	Br	Cl	Cl	3	40	20	600
31		Cl	Cl	H	OCF ₃	3	8	8	2,400
32		H	Br	H	OCF ₃	2	15	7	2,900

^aAverage value of duplicate experiments reported. ^bAverage value of triplicate experiments reported. ^cn.d. = value not determined.

Table 4. Rodent PK Parameters of 32

mouse ^a		rat ^b	
[plasma] (μM)	0.5 \pm 0.1	C _{max} (μM)	0.3
[liver] (μM)	5.9 \pm 1.1	T _{max} (h)	8.0
[muscle] (μM)	1.8 \pm 0.2	AUC _(0-t) ($\mu\text{M}\cdot\text{h}$)	5.8
[fat] (μM)	0.8 \pm 0.2	CL (mL h ⁻¹ kg ⁻¹)	574.8
		V _{ss} (L/kg)	19.3
		T _{1/2} (h)	25.3
		F (%)	88.1

^aMale C57BL6 mouse ($n = 3$), 10 mpk, po; data collected 24 h after dose. Values reported are the mean \pm SD. ^bFemale CD rat ($n = 3$), 5 mpk dose. The HCl salt of 32 dissolved in saline was used for both oral and iv formulations.

primarily responsible for glucose metabolism (liver, muscle, and fat) rather than in circulation.

Rat PK is also shown in Table 4. The plasma C_{max} after a 5 mpk dose was relatively low. The low clearance and high volume of distribution were in line with the desire to have systemic effects. The excellent oral bioavailability coupled with the long half-life further supported the advancement of 32, dosed once daily, into our PD models.

For our initial PD experiment, we measured the modulation of liver glycosphingolipid levels in mice after dosing with GCS inhibitors 32, 6, and 7. The ceramide species measured contained the C16 (palmitoyl) acyl chain. As is shown in Figure 4A, a 10 mpk dose of 32 was effective at significantly lowering glucosylceramide [$p < 0.05$ vs vehicle], lactosylceramide [$p < 0.05$ vs vehicle], and GM3 [$p < 0.05$ vs vehicle] levels. This effect was comparable to a 75 mpk dose of 7. Ceramide levels were unchanged from vehicle. Additionally, 32 was more potent than 6 in this experiment.¹⁷

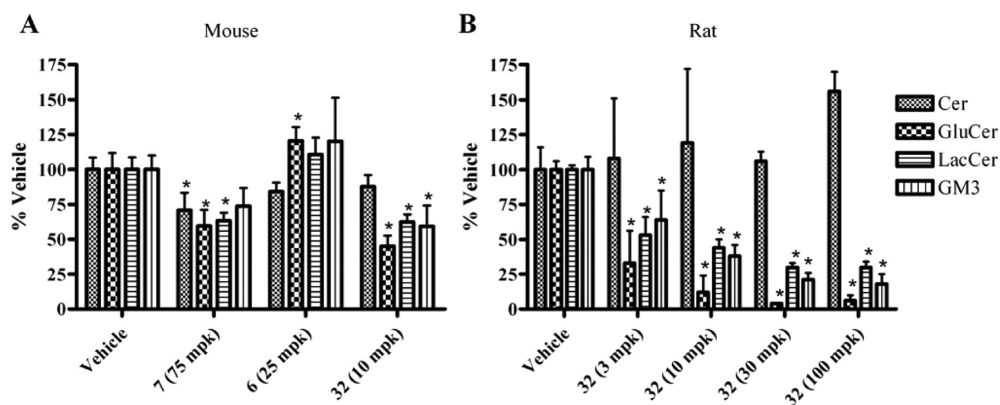
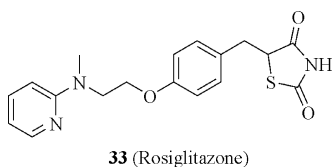


Figure 4. Effects of GCS inhibition on the liver levels of ceramide (Cer), glucosylceramide (GluCer), lactosylceramide (LacCer), and GM3 in lean mice (C57/B6, $n = 4$) after 4 days of dosing q.d., po (A). Data were collected 4 h after last dose. Data are presented as the mean \pm SD: (*) $p < 0.05$ vs vehicle, one-way ANOVA followed by Dunnett's test. Also shown are the effects of GCS inhibition in the livers of lean rats (Sprague–Dawley, $n = 3$) after 5 days of dosing (q.d., po) (B). Data were collected 24 h after last dose. Maximum GCS inhibition was observed at the 30 mpk dose (B). Data are depicted as the mean \pm SD: (*) $p < 0.05$ vs vehicle, one-way ANOVA followed by Dunnett's test.

While the mouse experiment was a promising snapshot of the ability of **32** to inhibit GCS in vivo, it was also necessary to find the dose at which maximum GCS inhibition could be maintained for 24 h after dose. The requisite dose response experiment was performed in rats (Figure 4B). Liver glycosphingolipid levels were measured 24 h after a 5-day regimen of 3, 10, 30, or 100 mpk doses. A clear dose response was observed for all measured signals downstream of GCS. Statistically significant decreases in glucosylceramide [$p < 0.05$ vs vehicle] were observed at all doses. This led to significant reductions in lactosylceramide [$p < 0.05$ vs vehicle] and GM3 [$p < 0.05$ vs vehicle]. The maximum effect was observed at the 30 mpk dose with no further benefit gained at 100 mpk. These results were used to determine dosing for the subsequent rodent efficacy experiments.

When **32** was dosed in diet induced obese (DIO) mice, robust glucose lowering and insulin sensitization were observed. Thiazolidinedione **33** (rosiglitazone), shown in Figure 5, was



33 (Rosiglitazone)

Figure 5. Positive control used for rodent efficacy experiments.

run as a positive control.¹⁸ A 10 mpk dose of **32**, once daily, increased oral glucose tolerance in 14 days (Figure 6A,B). After 28 days, **32** still significantly [$p < 0.05$] improved glucose tolerance (Figure 6C,D). These effects were observed without a confounding decrease in body weight (Figure 7A). Food intake was not measured. Fasting glucose was found to be significantly lower [$p < 0.05$], relative to vehicle treated control, after both 14 and 28 days of dosing (Figure 7B). Further evidence of increased insulin sensitivity was provided by an end of study measurement of insulin stimulated Akt phosphorylation (Figure 7C). Animals chronically treated with **32** and then given insulin had markedly increased pAkt [$p < 0.05$] relative to treatment naive animals. Increased pAkt implies increased insulin receptor function.¹⁹ These effects correlated well with decreased liver glycosphingolipid and GM3 levels measured at the end of the study (Figure 7D). The robust efficacy shown in this model inspired us to further characterize **32**.

After observing efficacy in the DIO mouse model, we looked for confirmation in a genetic diabetes model. For this experiment, we chose the Zucker diabetic fatty (ZDF) rat. **32** was administered orally, once daily, at either 10 or 30 mpk doses for 29 days (Figure 8). The first OGTT was performed after 15 days of dosing (Figure 8A,B). In this experiment, the 10 mpk dose did not have a significant effect. However, the 30 mpk dose improved glucose tolerance comparable to **33** [$p < 0.05$ vs ZDF vehicle]. A second OGTT, performed at 27 days, showed an improvement in efficacy at the 10 mpk dose of **32** (Figure 8C,D). This effect did not reach statistical significance. By 27 days, the 30 mpk dose of **32** nearly normalized glucose excursion and disposal in this model. However, the body weight data for this study were of concern (Figure 9A). Even though all the animals gained weight during the study, the compound **32** (30 mpk) dose group gained weight more slowly than the ZDF, vehicle treated controls. The decreased body weight gain was statistically significant [$p < 0.05$ vs ZDF vehicle] from day 7 onward. This decreased body weight gain was linked to decreased food intake.

Because this decreased body weight gain could have contributed to the efficacy signal measured in the OGTT, we opted to perform a pair-fed efficacy study. In this 29-day experiment, three ZDF control groups were used. One control group was fed ad libitum and dosed with vehicle. A second was pair-fed to the first control group and also dosed with vehicle. The third control group was pair-fed to the **32** (30 mpk) treated group and dosed with vehicle. After 14 days of dosing, HbA1c was measured (Figure 9B). Fortunately, the compound **32** group showed a statistically significant decrease relative to the pair-fed control group [$p < 0.06$ vs pair-fed vehicle].²⁰ This indicated to us that **32** was indeed improving glucose processing in this rat study. In addition, **32** had beneficial effects on lipid trafficking (Figure 9C). Decreased plasma triglycerides were observed relative to pair-fed control [$p < 0.05$ vs pair-fed vehicle]. In addition, abdominal fat pad mass was decreased relative to pair-fed controls [$p < 0.05$ vs pair-fed control] (Figure 9D).

Further evidence of decreased lipid accumulation mediated by **32** was found upon examination of liver samples. Livers were isolated from animals in both the ZDF rat and DIO mouse efficacy studies (Figure 10). When untreated, both of these animal models develop liver steatosis.²¹ The fat droplets in the

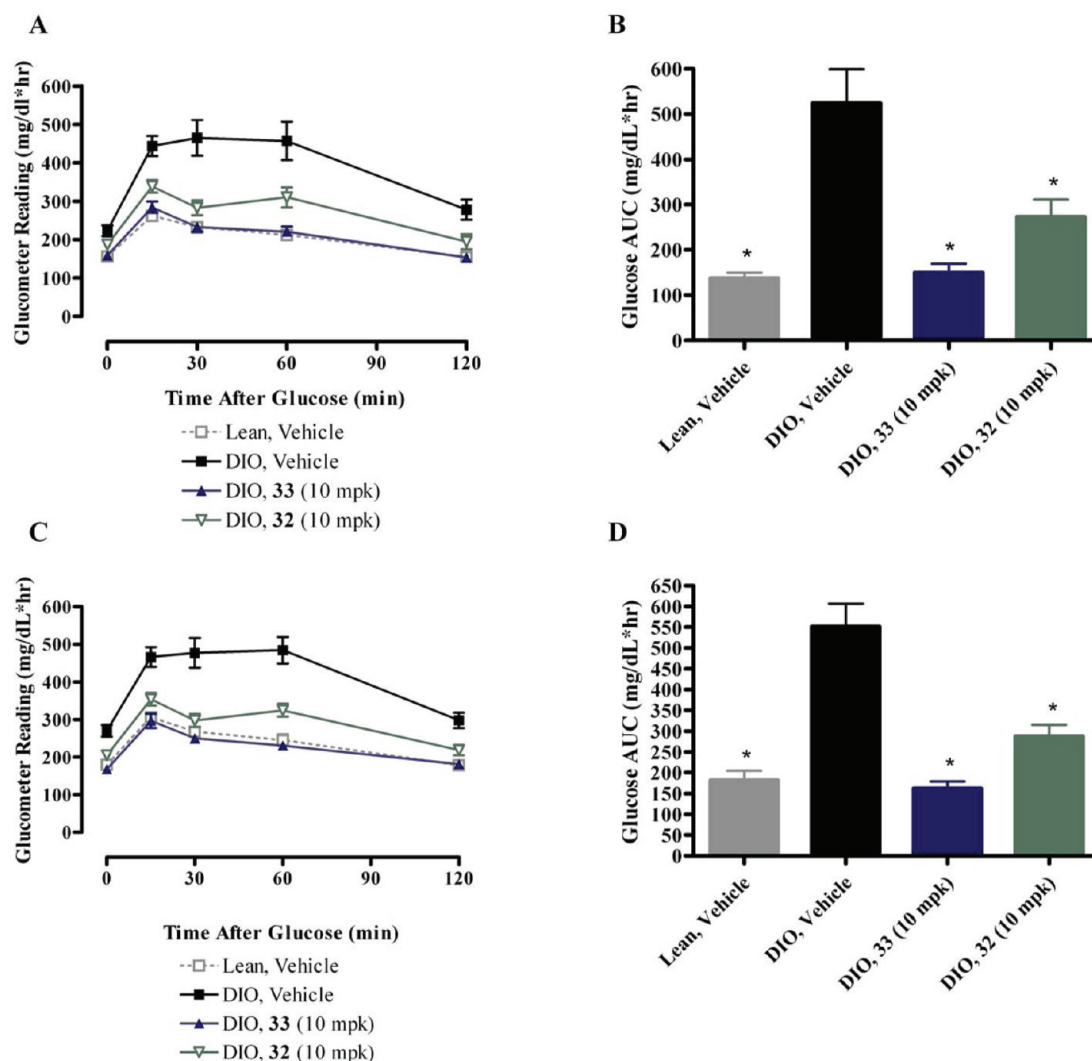


Figure 6. 32 was dosed once daily, by oral gavage, in diet induced obese (DIO) mice for 28 days ($n = 8$ per group). A control group was treated with 33. Day 14 OGTT (2 h after dose) data are presented. 32 dose group reached statistical significance [$p < 0.05$ vs DIO vehicle, two-way ANOVA followed by Bonferroni's test] at 15, 30, and 60 min time points. Lean vehicle and 33 groups were statistically different from DIO vehicle group at all measured time points [$p < 0.05$ vs DIO vehicle] (A). Also shown are day 14 AUC data with a glucose baseline of 135 mg/dL: (*) $p < 0.05$ vs DIO vehicle, one-way ANOVA followed by Dunnett's test (B). Day 28 OGTT (2 h after dose) data are presented. 32 dose group reached statistical significance [$p < 0.05$ vs DIO vehicle, two-way ANOVA followed by Bonferroni's test] at 15, 30, 60, and 120 min time points. Lean vehicle and 33 groups were statistically different from DIO vehicle group at all measured time points [$p < 0.05$ vs DIO vehicle, two-way ANOVA followed by Bonferroni's test] (C). Day 28 AUC data with a glucose baseline of 97 mg/dL are presented: (*) $p < 0.05$ vs DIO vehicle, one-way ANOVA followed by Dunnett's test (D).

hepatocytes were visualized using hematoxylin–eosin (H&E) and Oil Red O staining.²² The negative, or white, space in the H&E stained images generally represents fat. In the Oil Red O stained images, fat is red. The lean animal livers showed very little fat accumulation. In rat, the white spaces in the H&E stained images were not fat but sinusoidal tracts between hepatocytes. In contrast, the insulin resistant animals had marked fat accumulation. Four-week treatment with 32 showed decreased fat accumulation in both species. A quantitative measurement of this effect was not made.

We met our goal of finding a GCS inhibitor that had sufficient potency and exposure to achieve sustained target inhibition. Once daily dosing with compound 32 in rodent models resulted in decreased glucosylceramide and ganglioside levels. Robust efficacy, in the form of improved glucose tolerance in both DIO mice and ZDF rats, was observed after as

little as 2 weeks of dosing. Furthermore, decreased circulating triglycerides and fat pad mass and decreased liver fat accumulation were observed upon continued dosing. Thus, 32 represents further proof of the concept that GCS inhibition could be a viable treatment for type 2 diabetes.

CHEMISTRY

Preparation of hit 8a proceeded as described in Scheme 1. Activated BOC tryptophan (9) was subjected to EDC/HOBt mediated coupling with *N*-methylpiperazine. Following acidic BOC deprotection, the resulting amine was coupled with acid 14b, again under EDC/HOBt conditions. Benzylserine analogue 11 was prepared in a similar manner.

The phenylalanine analogues were prepared by one of two methods, both of which are described in Scheme 2. In the first approach, BOC phenylalanines 12a–d were coupled with

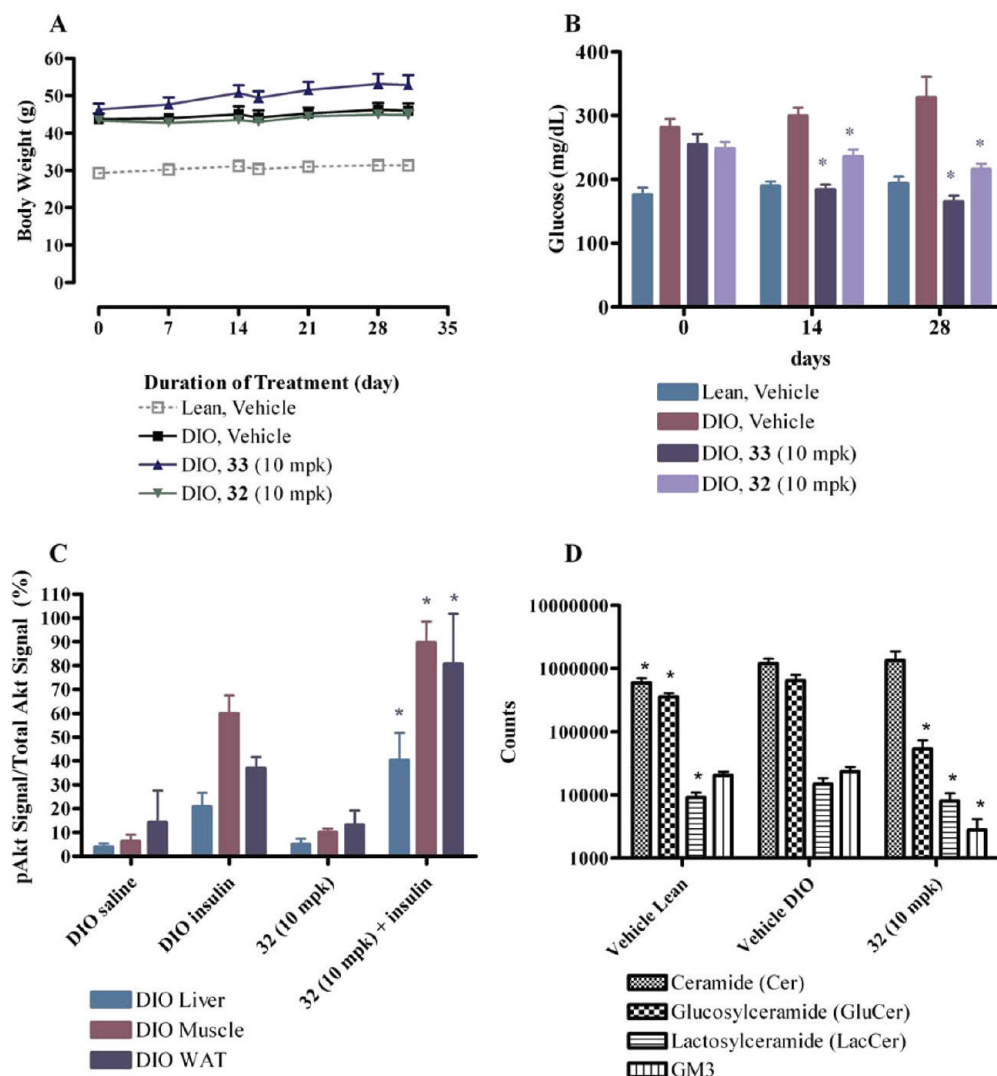


Figure 7. 32 was dosed once daily, by oral gavage, in diet induced obese (DIO) mice for 28 days ($n = 8$ per group). A control group was treated with 33. Shown is the body weight change over the course of the study. Data are depicted as the mean \pm SD (A). Fasted glucose measured at days 14 and 28 is shown: (*) $p < 0.05$ vs DIO vehicle, one-way ANOVA followed by Dunnett's test (B). Increased pAkt was observed 28 days after dosing in liver, fat, and muscle. Data are depicted as the mean \pm SD. For insulin naive 32 group, (*) $p < 0.05$ vs DIO saline control, one-way ANOVA followed by Bonferroni's test. For 32 + insulin group, (*) $p < 0.05$ vs DIO insulin group, one-way ANOVA followed by Bonferroni's test (C). End of study liver ceramide and glycosphingolipid levels were measured 24 h after final dose. Data are depicted as the mean \pm SD: (*) $p < 0.05$ vs DIO vehicle group, one-way ANOVA followed by Dunnett's test (D).

N-methylpiperazine using EDC/HOBt. BOC deprotection and coupling of the resulting amine with **14b** furnished analogues **17–20**. Alternatively, BOC phenylalanines **12b** and **12d** were esterified and deprotected to furnish amino esters **13a,b**. This was accomplished in two steps by EDC coupling with EtOH followed by HCl mediated cleavage of the BOC group. Or the esterification and deprotection were accomplished simultaneously by refluxing acids **12** in SOCl_2 . The amino esters **15a,b** were coupled, using either EDC/HOBt or HATU, to acids **14a,b**. Acid **14a** was prepared in two steps from **13a**. The arylacetonitrile **13a** was treated with NaH in THF, and the resulting anion was trapped with dibromoethane. Nitrile hydrolysis under forcing conditions provided the desired acid (**14a**). Ester hydrolysis and EDC coupling with R_1 amines provided analogues **24–26**. Final BOC deprotection with 4 M HCl in dioxane provided analogues **21–23** and **27–32**.

EXPERIMENTAL METHODS

Chemistry. All reagents and solvents were used as obtained from vendors unless specified in the text. Starting materials **12a–d** and **14b** were commercially available. Proton NMR spectra were collected using a Varian Mercury Plus 400 MHz spectrometer. Reported MS data were collected using a Waters Micromass ZQ or Agilent 1100 series MSD or similar instrument. All final compounds were at least 95% pure as determined by analytical HPLC (Waters Alliance or Shimadzu Prominence) using a Phenomenex Gemini C18 column ($50 \text{ mm} \times 4.60 \text{ mm}$, $3 \mu\text{m}$) or similar column.

1-(2,4-Dichlorophenyl)-*N*-[(2S)-3-(1*H*-indol-3-yl)-1-(4-methylpiperazin-1-yl)-1-oxopropan-2-yl]cyclopropanecarboxamide (8a**).** (*S*)-2,5-Dioxopyrrolidin-1-yl 2-(*tert*-butoxycarbonylamino)-3-(1*H*-indol-3-yl)propanoate (**9**) (Advanced Chemtech, 803 mg, 2 mmol) was dissolved in dry acetonitrile (10 mL). *N*-Methylpiperazine (233 μL , 2.1 mmol) was added and the solution stirred for 2 h. A complete reaction was indicated by LC/MS analysis. A 4 M solution of HCl in dioxane (2 mL) was added and the solution stirred overnight. A precipitate was formed that was filtered off and washed with acetonitrile. LC/MS analysis of the solid was consistent with the

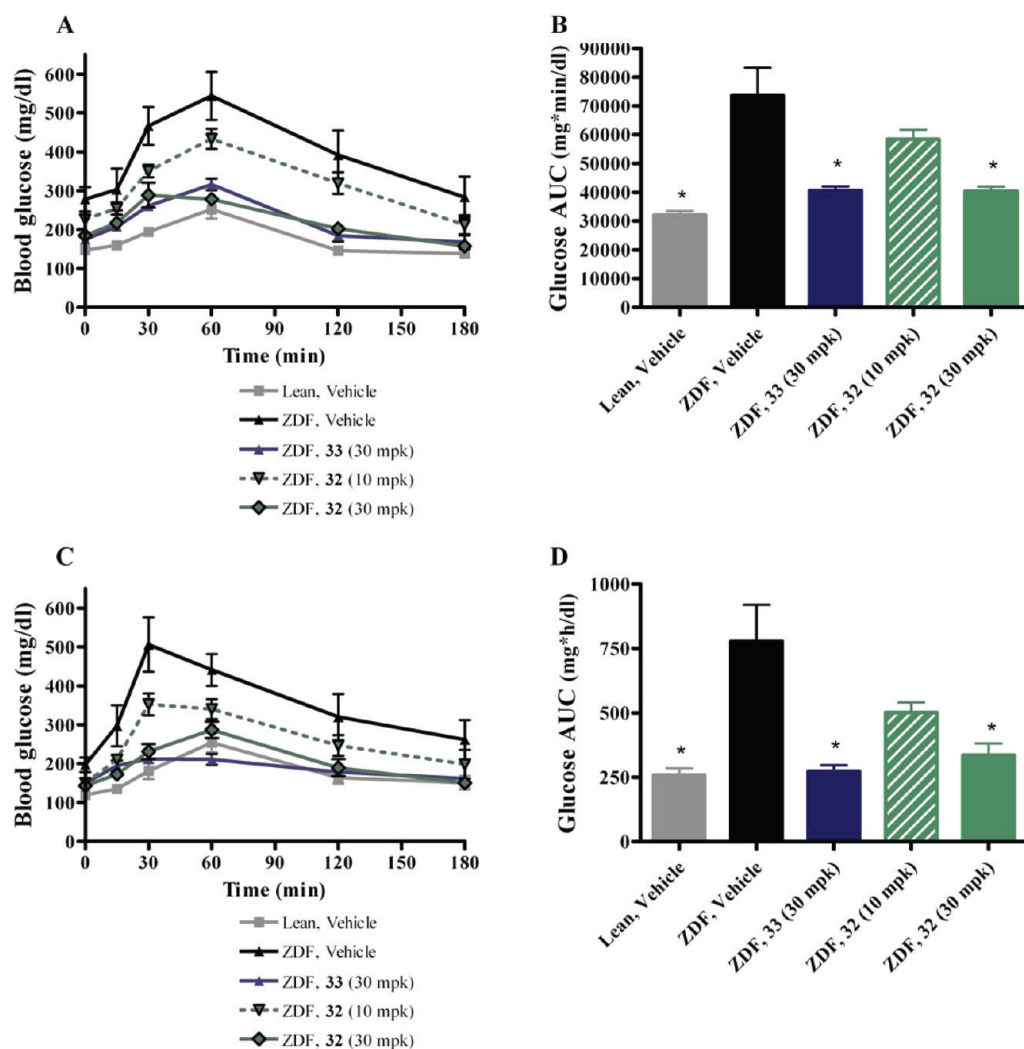


Figure 8. 32 was dosed once daily, by oral gavage, in Zucker diabetic fatty (ZDF) rats for 29 days ($n = 8$ per group). A control group was treated with 33. Shown are day 15 OGTT curves, 2 h after dose. 32 (10 mpk) dose group reached statistical significance [$p < 0.05$ vs ZDF vehicle, two-way ANOVA followed by Bonferroni's test] at 30 and 60 min time points. 32 (30 mpk) dose group reached statistical significance [$p < 0.05$ vs ZDF vehicle, two-way ANOVA followed by Bonferroni's test] at 30, 60, 120, and 180 min time points. 33 dose group reached statistical significance [$p < 0.05$ vs ZDF vehicle, two-way ANOVA followed by Bonferroni's test] at 30, 60, 120, and 180 min time points. Lean vehicle group was statistically different from ZDF vehicle group at all measured time points [$p < 0.05$ vs ZDF vehicle, two-way ANOVA followed by Bonferroni's test] (A). Day 15 AUC data are shown: (*) $p < 0.05$ vs ZDF vehicle, one-way ANOVA followed by Dunnett's test (B). Day 27 OGTT curves are shown, 2 h after dose. 32 10 mpk dose group reached statistical significance [$p < 0.05$ vs ZDF vehicle, two-way ANOVA followed by Bonferroni's test] at the 30 min time point. 32 30 mpk dose group reached statistical significance [$p < 0.05$ vs ZDF vehicle, two-way ANOVA followed by Bonferroni's test] at 15, 30, 60, 120, and 180 min time points. 33 dose group reached statistical significance [$p < 0.05$ vs ZDF vehicle, two-way ANOVA followed by Bonferroni's test] at 15, 30, 60, 120, and 180 min time points. Lean vehicle group was statistically different from ZDF vehicle group at 15, 30, 60, 120, and 180 min time points [$p < 0.05$ vs ZDF vehicle, two-way ANOVA followed by Bonferroni's test] (C). Day 27 OGTT AUC data with a glucose baseline of 145 mg/dL are shown: (*) $p < 0.05$ vs ZDF vehicle, one-way ANOVA followed by Dunnett's test (D).

mass of (*S*)-2-amino-3-(1*H*-indol-3-yl)-1-(4-methylpiperazin-1-yl)propan-1-one. After the sample was dried in vacuo, 690 mg of the amine was obtained (1.92 mmol of the monohydrochloride salt). This material was dissolved in dry acetonitrile (10 mL). Hünig's base (1.64 mL, 9.6 mmol), 1-(2,4-dichlorophenyl)cyclopropanecarboxylic acid (Acros, 443 mg, 1.92 mmol), and HATU (Applied Biosystems, 802 mg, 2.11 mmol) were added. The resulting reaction solution was stirred overnight. The product was isolated by reverse-phase preparative HPLC (aqueous ammonium acetate buffer solution, pH \approx 4–5, acetonitrile; 20–70% eluant gradient). Pure product containing fractions were collected, combined, concentrated, and lyophilized to obtain 466 mg (41%) of the title compound. $^1\text{H NMR}$ (400 MHz, $\text{DMSO-}d_6$): δ 10.84 (s, 1H), 7.61 (m, 1H), 7.41 (m, 1H), 7.35 (m, 2H), 7.31 (m, 1H), 7.04 (m, 1H), 7.01 (m, 1H), 6.85 (m, 1H), 6.68 (m, 1H), 5.93 (m, 1H), 3.25 (s, 3H), 3.08 (m, 1H),

2.95 (m, 2H), 2.17 (m, 1H), 2.09 (m, 1H), 2.05 (s, 3H), 1.94 (m, 1H), 1.70 (m, 1H), 1.45 (m, 2H), 0.97 (m, 2H). MS (EI) for $\text{C}_{26}\text{H}_{28}\text{Cl}_2\text{N}_4\text{O}_2$, found 499.0 (MH^+).

1-(2,4-Dichlorophenyl)-*N*-[1-(15)-2-(4-methylpiperazin-1-yl)-2-oxo-1-[[[phenylmethyl]oxy]methyl]ethyl]-cyclopropanecarboxamide (11). Compound 11 was prepared in an analogous manner to compound 8a. $^1\text{H NMR}$ (400 MHz, $\text{DMSO-}d_6$): δ 7.66 (d, 1H), 7.47 (m, 2H), 7.34 (m, 2H), 7.29 (m, 1H), 7.23 (m, 2H), 6.85 (d, 1H), 4.92 (m, 1H), 4.41 (m, 2H), 3.49 (m, 6H), 2.43 (m, 4H), 2.29 (s, 3H), 1.49 (m, 2H), 1.04 (m, 2H). MS (EI) for $\text{C}_{25}\text{H}_{29}\text{Cl}_2\text{N}_3\text{O}_3$, found 491 (MH^+).

1-(4-(Trifluoromethoxy)phenyl)cyclopropanecarboxylic Acid (14a). NaH (60% in mineral oil, 14.9 g, 372 mmol) was added to a dry flask. The flask was cooled in an ice bath, and THF (100 mL) was added. The slurry was stirred for \sim 5 min. To that slurry was added a solution of 2-(4-(trifluoromethoxy)phenyl)acetonitrile (13a)

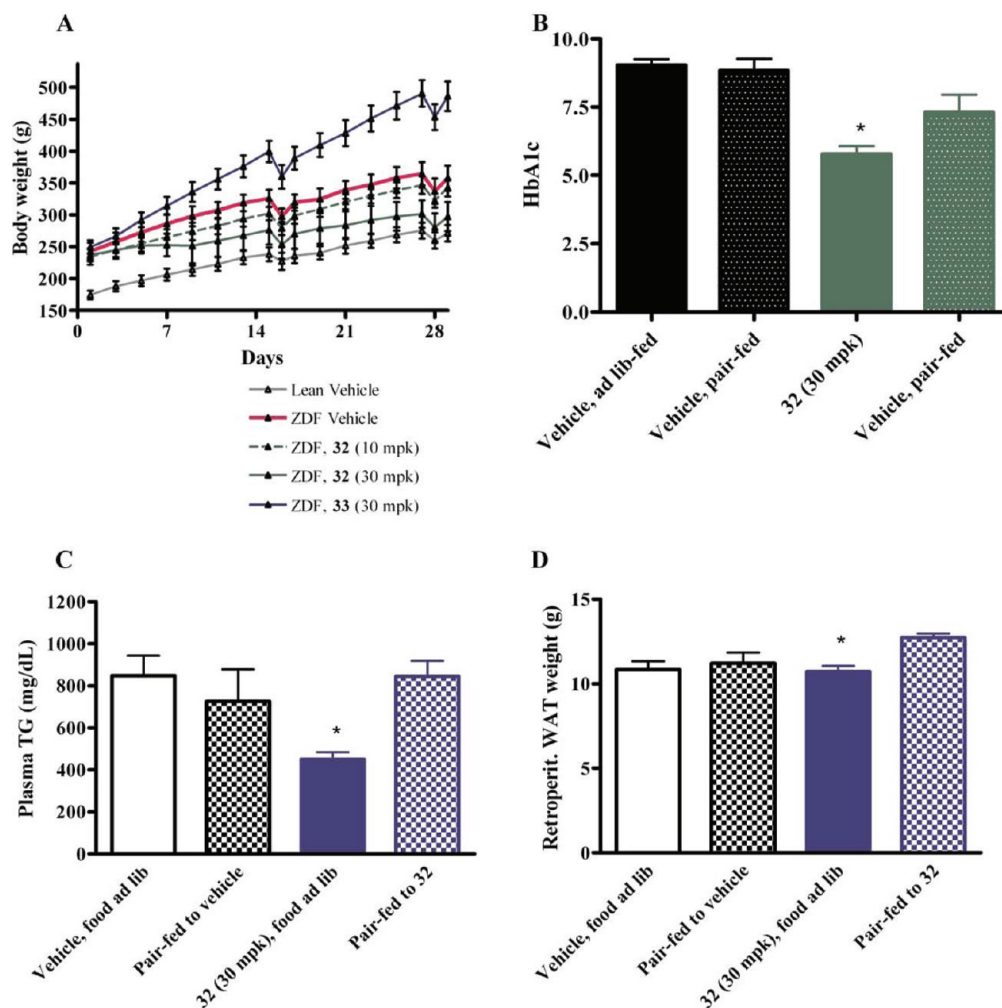


Figure 9. 32 was dosed once daily, by oral gavage, in Zucker diabetic fatty (ZDF) rats for 29 days ($n = 8$ per group). Body weight change over the course of the study is shown. Data are depicted as the mean \pm SEM. 32 (30 mpk) dose group was statistically different from ZDF vehicle group from day 7 onward [$p < 0.05$ vs ZDF vehicle, two-way ANOVA followed by Bonferroni's test]. 33 dose group was statistically different from ZDF vehicle group from day 7 onward [$p < 0.05$ vs ZDF vehicle, two-way ANOVA followed by Bonferroni's test] (A). Shown are results from day 14 HbA1c analysis, pair-fed ZDF efficacy experiment with 30 mpk 32: (*) $p < 0.06$ vs ZDF pair-fed vehicle, one-way ANOVA followed by Bonferroni's test (B). Plasma triglyceride levels following 28 days of dosing with 32 at 30 mpk (ZDF rats, pair-fed) are shown: (*) $p < 0.05$ vs pair-fed vehicle, one-way ANOVA followed by Bonferroni's test (C). Retroperitoneal WAT weight is shown following 28 days of dosing with 32 at 30 mpk (ZDF rats, pair-fed): (*) $p < 0.05$ vs pair-fed vehicle, one-way ANOVA followed by Bonferroni's test (D).

(25 g, 124 mmol) in 120 mL of THF via dropping funnel. The resulting mixture was warmed to room temperature and stirred for 40 min before cooling again in an ice bath. Dibromoethane (70 g, 372 mmol) was added dropwise via syringe. The reaction mixture was warmed to room temperature and stirred overnight. The reaction was quenched by the addition of 1 M HCl and extracted with EtOAc. The organics were washed with water and brine and dried with MgSO_4 . The solvent was removed, and the residue was used crude in the next step. To a solution of NaOH (35 g, 795 mmol) in 400 mL of water was added 1-(4-(trifluoromethoxy)phenyl)cyclopropanecarbonitrile (14.9 g, 65.0 mmol). The reaction mixture was heated to 120 °C for 48 h. The resulting solution was cooled to 0 °C and acidified to pH 3 via addition of concentrated HCl. The resulting precipitate was filtered, washed with water, and dried. The dry residue was redissolved in diethyl ether (500 mL), filtered from salts, and concentrated under reduced pressure. The resulting off-white solid was used in the next step without further purification (15.6 g, 97.5%). $^1\text{H NMR}$ (400 MHz, $\text{DMSO}-d_6$): δ 12.47 (m, 1H), 7.68–7.34 (m, 2H), 7.25 (m, 2H), 1.45 (m, 2H), 1.29–0.91 (m, 2H). MS (EI) for $\text{C}_{11}\text{H}_9\text{F}_3\text{O}_3$, found 247.2 (MH^+).

(S)-Ethyl 2-Amino-3-(2,4-dichlorophenyl)propanoate (15a). To a solution of (S)-2-(*tert*-butoxycarbonylamino)-3-(2,4-

dichlorophenyl)propanoic acid (**10b**) (5 g, 15 mmol, Fluka) in dichloromethane (100 mL) were added 1-hydroxybenzotriazole (3 g, 22.5 mmol), *N*-methylmorpholine (16.5 mL, 150 mmol), 1-[3-(dimethylamino)propyl]-3-ethylcarbodiimide hydrochloride (4.3 g, 22.8 mmol), and ethyl alcohol (13.8 mL, 300 mmol). The mixture was stirred at room temperature for 18 h. The resulting solution was extracted with water (25 mL), saturated sodium bicarbonate solution (25 mL), and 1 M HCl solution (25 mL). The layers were separated, and the organic layer was dried over MgSO_4 , filtered, and concentrated in vacuo. The resulting oil was dissolved in methanol (25 mL) followed by the addition of 4 M HCl in dioxane (25 mL, Aldrich). The mixture was stirred at room temperature for 18 h. The resulting solution was concentrated in vacuo to give 3.0 g (60%) of the title compound which was used in the next step without further purification. $^1\text{H NMR}$ (400 MHz, $\text{DMSO}-d_6$): δ 8.86 (s, 3H), 7.65 (m, 1H), 7.46 (m, 2H), 4.14 (m, 1H), 4.13–3.92 (m, 2H), 3.53–3.02 (m, 2H), 1.05 (m, 3H). MS (EI) for $\text{C}_{11}\text{H}_{13}\text{Cl}_2\text{NO}_2$, found 263.2 (MH^+).

(S)-Ethyl 2-Amino-3-(4-bromophenyl)propanoate (15b). To a solution of BOC-L-4-bromophenylalanine (**10d**) (30.0 g, 87.16 mmol, Chem-Impex) in ethanol (450 mL) was added thionyl chloride (8.0 mL, 109.67 mmol). The mixture was warmed at 90 °C for 18 h.

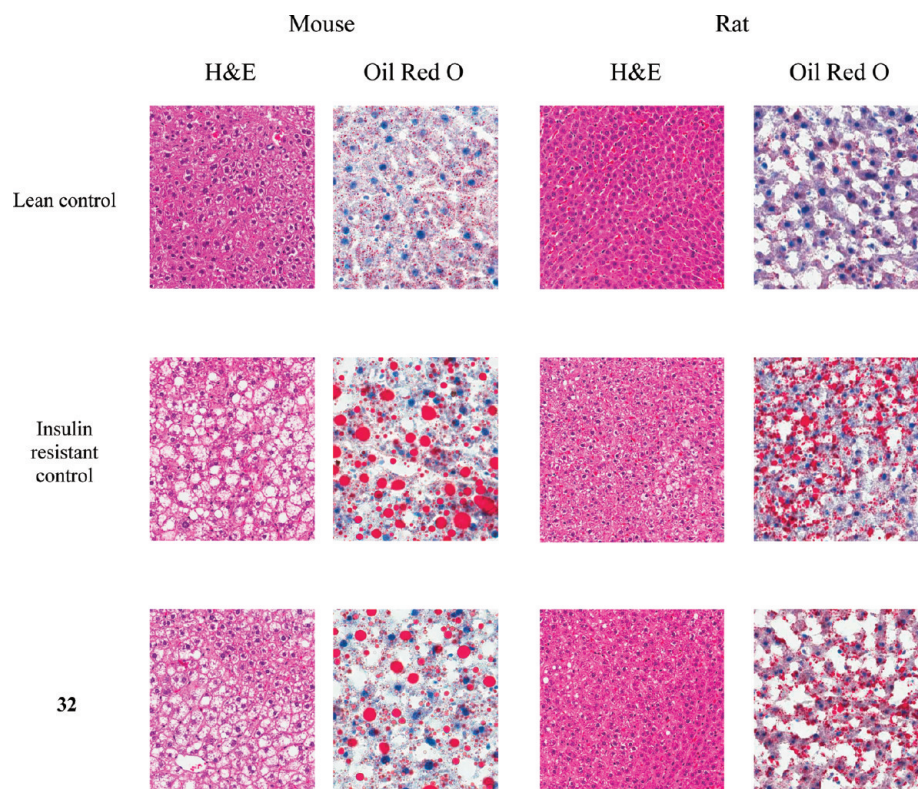
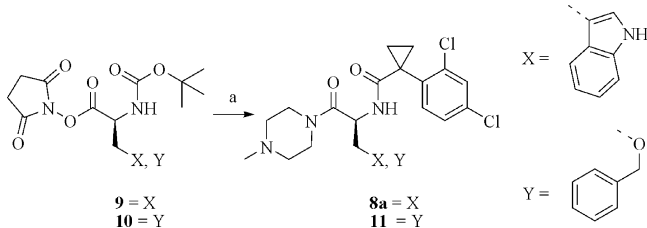


Figure 10. Liver preparation and staining from DIO mouse and ZDF rat efficacy experiments. With hematoxylin–eosin (H&E) stain, nuclei appear blue and fat droplets white. With Oil Red O stain, nuclei appear blue and fat droplets stain red. After 4 weeks of treatment, 32 showed a qualitative decrease in fat accumulation.

Scheme 1^a



^aReagents and conditions: (a) (i) *N*-methylpiperazine, MeCN, rt, 2 h; (ii) 4 M HCl in dioxane, rt, 18 h; (iii) **14b**, HATU, MeCN, Hünig's base, rt, 18 h.

The resulting solution was concentrated in vacuo to give 27.0 g (90%) of the title compound as the HCl salt which was used in the next step without further purification. ¹H NMR (400 MHz, DMSO-*d*₆): δ 8.76 (s, 3H), 7.53 (m, 2H), 7.24 (m, 2H), 4.23 (m, 1H), 4.16–4.00 (m, 2H), 3.15 (m, 2H), 1.12 (m, 3H). MS (EI) for C₁₁H₁₄BrNO₂, found 273.1 (MH⁺).

(S)-3-(4-Bromophenyl)-2-(1-(4-(trifluoromethoxy)phenyl)cyclopropanecarboxamido)propanoic Acid (16d). To a solution of (*S*)-ethyl 2-amino-3-(4-bromophenyl)propanoate (**15b**) (11.5 g, 42.26 mmol) in acetonitrile (150.0 mL) were added 1-(4-(trifluoromethoxy)phenyl)cyclopropanecarboxylic acid (**14a**) (10.4 g, 42.26 mmol), Hünig's base (13.9 mL, 84.52 mmol), and HATU (19.3 g, 50.71 mmol). The mixture was stirred at room temperature for 1 h. The resulting solution was concentrated in vacuo, dissolved in dichloromethane (350 mL), and extracted with water (350 mL) 2 times. The layers were separated, and the organic layer was dried over MgSO₄. The resulting solution was concentrated in vacuo and chromatographed on silica gel, eluting with 15% EtOAc in hexane to give 17.4 g (82%) of (*S*)-ethyl 3-(4-bromophenyl)-2-(1-(4-trifluoromethoxy)phenyl)cyclopropanecarboxamido)propanoate. ¹H

NMR (400 MHz, DMSO-*d*₆): δ 7.44 (m, 2H), 7.36–7.21 (m, 4H), 7.08 (m, 3H), 4.44 (m, 1H), 4.04 (m, 2H), 3.11–2.79 (m, 2H), 1.31–1.21 (m, 2H), 1.17–1.07 (m, 3H), 1.06–0.88 (m, 2H). MS (EI) for C₂₂H₂₁BrF₃NO₄, found 501.3 (MH⁺). To a solution of the ester (17.4 g, 34.8 mmol) in 300 mL of MeOH was added 100 mL of 2 N NaOH solution, and the reaction mixture was stirred at room temperature for 18 h. The resulting solution was concentrated under reduced pressure, acidified with concentrated HCl to pH 3, and extracted with 300 mL of EtOAc. The organic layer was dried over MgSO₄, filtered, and concentrated in vacuo to give 14.5 g (88%) of the title compound which was used in the next step without further purification. ¹H NMR (400 MHz, DMSO-*d*₆): δ 12.57 (s, 1H), 7.44 (m, 2H), 7.34–7.16 (m, 4H), 7.04 (m, 2H), 6.87 (m, 1H), 4.42 (m, 1H), 3.09–2.68 (m, 2H), 1.25 (m, 2H), 1.10–0.80 (m, 2H). MS (EI) for C₂₀H₁₇BrF₃NO₄, found 473.3 (MH⁺).

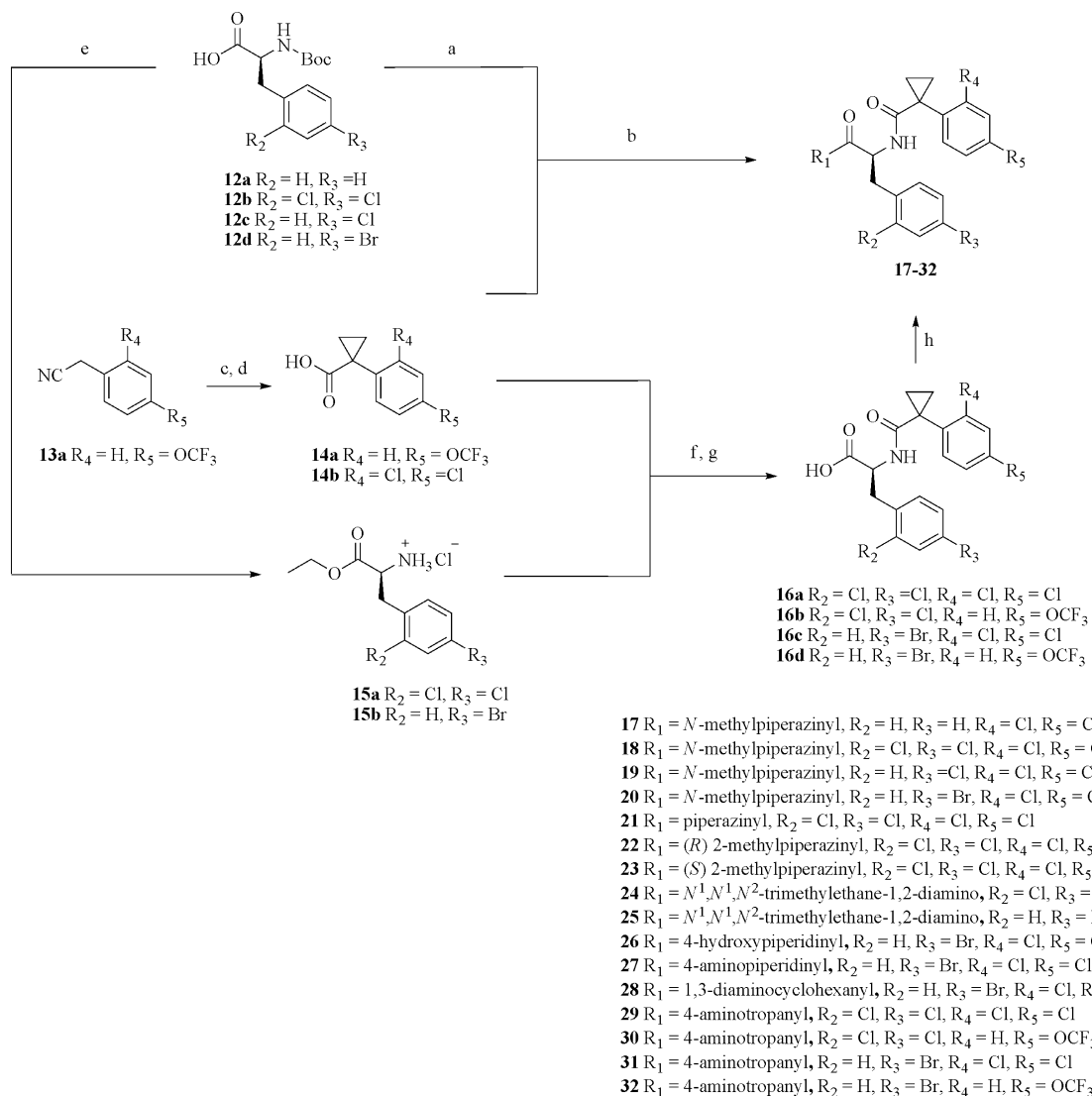
Compounds **16a–c** were made in an analogous manner to **16d**.

(S)-3-(2,4-Dichlorophenyl)-2-(1-(2,4-dichlorophenyl)cyclopropanecarboxamido)propanoic Acid (16a). ¹H NMR (400 MHz, DMSO-*d*₆): δ 12.73 (s, 1H), 7.62–7.46 (m, 1H), 7.37 (m, 3H), 7.17 (m, 1H), 6.99 (d, 1H), 4.50 (m, 1H), 3.17 (m, 1H), 2.92 (m, 1H), 1.49–1.11 (m, 2H), 1.06–0.79 (m, 2H). MS (EI) for C₁₉H₁₅Cl₄NO₃, found 448.5 (MH⁺).

(S)-3-(2,4-Dichlorophenyl)-2-(1-(4-(trifluoromethoxy)phenyl)cyclopropanecarboxamido)propanoic Acid (16b). ¹H NMR (400 MHz, DMSO-*d*₆): δ 12.65 (s, 1H), 7.52 (m, 1H), 7.45–7.28 (m, 5H), 7.16 (m, 2H), 4.70–4.35 (m, 1H), 3.25–2.83 (m, 2H), 1.33–1.08 (m, 2H), 1.08–0.70 (m, 2H). MS (EI) for C₂₀H₁₆Cl₂F₃NO₄, found 461.9 (MH⁺).

(S)-3-(4-Bromophenyl)-2-(1-(2,4-dichlorophenyl)cyclopropanecarboxamido)propanoic Acid (16c). ¹H NMR (400 MHz, DMSO-*d*₆): δ 7.60–7.52 (m, 1H), 7.44–7.31 (m, 4H), 7.03 (m, 2H), 6.73 (d, 1H), 4.38 (m, 1H), 3.05–2.75 (m, 2H), 1.42–1.29 (m, 2H), 1.07–0.83 (m, 2H).

1-(2,4-Dichlorophenyl)-*N*-[(1S)-2-(4-methylpiperazin-1-yl)-2-oxo-1-(phenylmethyl)ethyl]cyclopropanecarboxamide (17). To a solution of **10a** (2.7 g, 10 mmol) dissolved in dichloromethane

Scheme 2^a

^aReagents and conditions: (a) (i) *N*-methylpiperazine, EDC, HOBT, *N*-methylmorpholine, CH₂Cl₂, rt, 18 h; (ii) 4 M HCl in dioxane; (b) *N*-methylpiperazine, EDC, HOBT, *N*-methylmorpholine, CH₂Cl₂, rt, 18 h; (c) NaH, 1,2-dibromoethane, THF, 0 °C to rt, 18 h; (d) NaOH, water, 120 °C, 48 h; (e) (i) EtOH, EDC, HOBT, *N*-methylmorpholine, rt, 18 h; (ii) 4 M HCl in dioxane or SOCl₂, EtOH, 90 °C, 18 h; (f) EDC, HOBT, *N*-methylmorpholine, CH₂Cl₂, rt, 18 h or HATU, Hünig's base, MeCN, rt, 1 h; (g) 2 M NaOH, MeOH, rt, 18 h; (h) (i) amine, EDC, HOBT, *N*-methylmorpholine, CH₂Cl₂, rt, 18 h; (ii) 4 M HCl in dioxane.

(50 mL) were added 1-hydroxybenzotriazole (1.8 g, 13.7 mmol), Hünig's base (2 mL, 12.2 mmol), and 1-[3-(dimethylamino)propyl]-3-ethylcarbodiimide hydrochloride (2.3 g, 12.2 mmol). After the mixture was stirred for 10 min, *N*-methylpiperazine (1.2 mL, 11 mmol) was added. The resulting solution was stirred for 18 h and was then diluted with water and dichloromethane. The organic layer was separated and dried over MgSO₄. The solvent was removed, and the residue was dissolved in EtOAc (50 mL). To this solution was added 4 M HCl in dioxane (50 mL). The resulting solution was stirred at room temperature for an additional 18 h. The solvents were removed, and the residue was used without purification. Then 100 mg (0.3 mmol) of this residue was dissolved in DMF (2 mL). To this solution were added 1-[3-(dimethylamino)propyl]-3-ethylcarbodiimide hydrochloride (86 mg, 0.5 mmol), 1-hydroxybenzotriazole (69 g, 0.5 mmol), Hünig's base (0.5 mL, 3.1 mmol), and **14a** (70 mg, 0.3 mmol). The reaction mixture was stirred at room temperature for 18 h. The resulting solution was extracted with water (25 mL), saturated sodium bicarbonate (25 mL), and 1 M HCl (25 mL). The organic layer was separated and dried over MgSO₄. The resulting solution was concentrated in vacuo and purified by preparative HPLC to provide

369 mg (8%) of the title compound. ¹H NMR (400 MHz, DMSO-*d*₆): δ 7.51 (s, 1H), 7.44–7.34 (m, 2H), 7.30–7.20 (m, 3H), 7.13–7.08 (m, 1H), 6.57 (m, 1H), 5.09–5.00 (m, 1H), 3.64–3.48 (m, 3H), 2.88 (m, 2H), 2.65–2.47 (m, 3H), 2.23–2.15 (m, 1H), 1.63–1.52 (m, 2H), 1.18–1.04 (m, 2H). MS (EI) for C₂₄H₂₇Cl₂N₃O₂, found 461.9 (MH⁺).

Compounds **18–20** were made in an analogous manner to compound **17**.

1-(2,4-Dichlorophenyl)-*N*-[1-(2,4-dichlorophenyl)methyl]-2-(4-methylpiperazin-1-yl)-2-oxoethyl]-cyclopropanecarboxamide (18). ¹H NMR (400 MHz, CD₃OD): δ 7.51 (m, 1H), 7.48–7.35 (m, 3H), 7.35 (m, 1H), 7.15 (m, 1H), 5.18 (m, 1H), 3.78–3.63 (m, 2H), 3.58–3.44 (m, 2H), 3.05 (m, 1H), 2.96 (m, 1H), 2.78–2.55 (m, 4H), 1.58–1.43 (m, 2H), 1.13–1.10 (m, 2H). MS (EI) for C₂₄H₂₅Cl₄N₃O₂, found 530 (MH⁺).

***N*-[1-(4-Chlorophenyl)methyl]-2-(4-methylpiperazin-1-yl)-2-oxoethyl]-1-(2,4-dichlorophenyl)-cyclopropanecarboxamide (19)**. ¹H NMR (400 MHz, DMSO-*d*₆): δ 0.763 (s, 1H), 7.40 (s, 2H), 7.26 (m, 2H), 7.09 (m, 2H), 6.83 (m, 1H), 4.87 (m, 1H), 3.46–3.25 (m, 4H), 2.86–2.73 (m, 2H),

2.19–2.02 (m, 7H), 1.42–1.29 (m, 2H), 0.98–0.89 (m, 2H). MS (EI) for $C_{24}H_{26}Cl_3N_3O_2$, found 495.8 (MH⁺).

N-[(1S)-1-[(4-Bromophenyl)methyl]-2-(4-methylpiperazin-1-yl)-2-oxoethyl]-1-(2,4-dichlorophenyl)cyclopropanecarboxamide (20). ¹H NMR (400 MHz, DMSO-*d*₆): δ 7.63 (s, 1H), 7.43 (m, 4H), 7.05 (m, 2H), 6.86 (m, 1H), 4.90 (m, 1H), 3.46–3.33 (m, 4H), 2.86–2.73 (m, 2H), 2.24–2.10 (m, 7H), 1.44–1.34 (m, 2H), 1.01–0.96 (m, 2H). MS (EI) for $C_{24}H_{26}BrCl_2N_3O_2$, found 540.3 (MH⁺).

4-Bromo-N-α-[[1-(2,4-dichlorophenyl)cyclopropyl]carbonyl]-N-[2-(dimethylamino)ethyl]-N-methyl-L-phenylalaninamide (25). To a solution of (S)-3-(4-bromophenyl)-2-(1-(2,4-dichlorophenyl)cyclopropanecarboxamido)propanoic acid (16c) (87 mg, 0.19 mmol) in dichloromethane (5 mL) were added 1-hydroxybenzotriazole (25 mg, 0.19 mmol), N-methylmorpholine (0.172 mL, 1.57 mmol), 1-[3-(dimethylamino)propyl]-3-ethylcarbodiimide hydrochloride (36 mg, 0.19 mmol), and N¹,N¹-dimethylethane-1,2-diamine (16 mg, 0.19 mmol, TCI America). The mixture was stirred at room temperature for 18 h. The resulting solution was washed with water (25 mL) and saturated sodium bicarbonate (25 mL). The layers were separated, and the organic layer was dried over MgSO₄, filtered, and concentrated in vacuo. The product was then purified by preparative HPLC (reverse-phase, acetonitrile/aqueous 10 mM formic acid buffer) to give 41 mg (40%) of the title compound. ¹H NMR (400 MHz, DMSO-*d*₆): δ 8.16 (s, 1H), 7.60 (m, 1H), 7.46–7.34 (m, 4H), 7.08–6.98 (m, 2H), 4.84 (m, 1H), 3.45 (m, 1H), 3.25–3.08 (m, 1H), 2.93 (s, 2H), 2.85–2.70 (m, 3H), 2.37–2.20 (m, 2H), 2.21–2.08 (m, 6H), 1.43–1.29 (m, 2H), 1.03–0.88 (m, 2H). MS (EI) for $C_{24}H_{28}BrCl_2N_3O_2$, found 542.3 (MH⁺).

Compounds 24 and 26 were made in an analogous manner to compound 25.

2,4-Dichloro-N-α-[[1-(2,4-dichlorophenyl)cyclopropyl]carbonyl]-N-[2-(dimethylamino)ethyl]-N-methyl-L-phenylalaninamide (24). ¹H NMR (400 MHz, DMSO-*d*₆): δ 8.18 (s, 1H), 7.58 (m, 1H), 7.51 (m, 1H), 7.42 (m, 2H), 7.33 (m, 1H), 7.23 (m, 1H), 4.99 (m, 1H), 3.40 (m, 1H), 3.23 (m, 1H), 2.95 (s, 3H), 2.86 (m, 2H), 2.27 (m, 2H), 2.13 (s, 6H), 1.37 (m, 1H), 1.14 (m, 1H), 0.96 (m, 1H), 0.89 (m, 1H). MS (EI) for $C_{24}H_{27}Cl_4N_3O_2$, found 532.4 (MH⁺).

N-[(1S)-1-[(4-Bromophenyl)methyl]-2-(4-hydroxypiperidin-1-yl)-2-oxoethyl]-1-(2,4-dichlorophenyl)cyclopropanecarboxamide (26). ¹H NMR (400 MHz, DMSO-*d*₆): δ 7.61 (m, 1H), 7.40 (m, 4H), 7.01 (m, 2H), 6.75 (m, 1H), 4.88 (m, 1H), 4.74 (m, 1H), 3.86 (m, 1H), 3.84–3.56 (m, 4H), 3.19–2.63 (m, 2H), 1.60 (m, 2H), 1.40–1.11 (m, 7H), 0.96 (m, 2H). MS (EI) for $C_{24}H_{25}BrCl_2N_3O_3$, found 541.0 (MH⁺).

N-[(1S)-2-(3-Amino-8-azabicyclo[3.2.1]oct-8-yl)-1-[(4-bromophenyl)methyl]-2-oxoethyl]-1-[4-[(trifluoromethyl)oxy]phenyl]cyclopropanecarboxamide (32). To a solution of (S)-3-(4-bromophenyl)-2-(1-(4-(trifluoromethoxy)phenyl)cyclopropanecarboxamido)propanoic acid (16d) (100 mg, 0.2 mmol) in acetonitrile (5.0 mL) were added *tert*-butyl 8-azabicyclo[3.2.1]octan-3-ylcarbamate (Oakwood, 45.2 mg, 0.2 mmol), Hünig's base (1.1 mL, 6.1 mmol), and HATU (76 mg, 0.2 mmol). The mixture was stirred at room temperature for 1 h. The resulting solution was concentrated in vacuo. The residue was dissolved in dichloromethane (300 mL). This organic solution was extracted with water (10 mL), saturated sodium bicarbonate (10 mL), and saturated sodium chloride (10 mL). The layers were separated, and the organic layer was dried over MgSO₄, filtered, and concentrated in vacuo. The resulting oil was dissolved in methanol (10 mL), and 4 M HCl in dioxane (5 mL, Aldrich) was added. The mixture was heated to 45 °C for 2 h. The resulting solution was concentrated in vacuo. The product was purified by preparative HPLC (reverse-phase, acetonitrile/water with 0.1% formic acid) to give 20 mg (17%) of the title compound. Analytical HPLC: YMC Pack Pro 150 mm × 4.6 mm, 5 μm C18 column; 10–90% MeCN (0.1% TFA) in H₂O (0.1% TFA); flow rate 1.5 mL/min × 25 min; retention time of 14.37 min at 254 nm. ¹H NMR (400 MHz, DMSO-*d*₆): δ 7.42 (m, 2H), 7.31 (m, 4H), 7.03 (m, 3H), 4.67 (m, 1H), 4.27 (m, 2H), 3.10 (m, 1H), 2.78 (m, 2H), 1.81 (m, 8H), 1.22 (m, 2H), 0.98 (m, 2H). MS (EI) for $C_{27}H_{29}BrF_3N_3O_3$, found 581.4 (MH⁺).

Compounds 21–23 and 27–31 were made in an analogous manner to compound 32.

1-(2,4-Dichlorophenyl)-N-[(1S)-1-[(2,4-dichlorophenyl)methyl]-2-oxo-2-piperazin-1-ylethyl]-cyclopropanecarboxamide (21). ¹H NMR (400 MHz, DMSO-*d*₆): δ 8.24 (s, 1H), 7.62 (m, 1H), 7.53 (m, 1H), 7.45–7.40 (m, 1H), 7.37–7.35 (m, 1H), 7.23 (m, 1H), 6.94 (m, 1H), 5.04–4.98 (m, 1H), 3.43–3.29 (m, 5H), 2.97–2.84 (m, 2H), 2.67–2.51 (m, 4H), 1.41–1.36 (m, 1H), 1.21–1.18 (m, 1H), 0.97–0.90 (m, 2H). MS (EI) for $C_{23}H_{23}Cl_4N_3O_2$, found 516.1 (MH⁺).

1-(2,4-Dichlorophenyl)-N-[(1S)-1-[(2,4-dichlorophenyl)methyl]-2-[(3R)-3-methylpiperazin-1-yl]-2-oxoethyl]-cyclopropanecarboxamide (22). ¹H NMR (400 MHz, CD₃OD): δ 8.43 (s, 1H), 7.50–7.38 (m, 4H), 7.25–7.15 (m, 2H), 7.20–7.15 (m, 1H), 4.35 (m, 1H), 4.00 (m, 1H), 3.25–2.80 (m, 7H), 1.57–1.43 (m, 2H), 1.20–1.05 (m, 2H). MS (EI) for $C_{24}H_{25}Cl_4N_3O_2$, found 529.9 (MH⁺).

1-(2,4-Dichlorophenyl)-N-[(1S)-1-[(2,4-dichlorophenyl)methyl]-2-[(3S)-3-methylpiperazin-1-yl]-2-oxoethyl]-cyclopropanecarboxamide (23). ¹H NMR (400 MHz, CD₃OD): δ 8.42 (s, 1H), 7.53–7.39 (m, 4H), 7.33–7.13 (m, 2H), 5.20–5.15 (m, 1H), 4.40 (m, 1H), 4.02 (m, 1H), 3.25–2.84 (m, 6H), 2.80–2.58 (m, 1H), 1.55–1.40 (m, 2H), 1.23–1.00 (m, 5H). MS (EI) for $C_{24}H_{25}Cl_4N_3O_2$, found 530.1 (MH⁺).

N-[(1S)-2-(4-Aminopiperidin-1-yl)-1-[(4-bromophenyl)methyl]-2-oxoethyl]-1-(2,4-dichlorophenyl)cyclopropanecarboxamide (27). ¹H NMR (400 MHz, CD₃OD): δ 8.37 (s, 1H), 7.58 (d, 1H), 7.40–7.35 (m, 3H), 7.00–6.90 (m, 2H), 4.85–4.80 (m, 1H), 4.18–4.05 (m, 2H), 3.86–3.78 (m, 2H), 3.05–2.85 (m, 2H), 2.80–2.68 (m, 3H), 1.80–1.73 (m, 2H), 1.37–1.00 (m, 3H), 0.95–0.86 (m, 2H). MS (EI) for $C_{24}H_{26}BrCl_2N_3O_2$, found 540.1 (MH⁺).

N-(3-Aminocyclohexyl)-2,4-dichloro-N-α-[[1-(2,4-dichlorophenyl)cyclopropyl]carbonyl]-L-phenylalaninamide (28). ¹H NMR (400 MHz, CD₃OD): δ 8.52 (s, 1H), 7.50–7.38 (m, 4H), 7.23–7.15 (m, 2H), 4.82–4.75 (m, 1H), 3.67–3.58 (m, 1H), 2.20–2.13 (m, 1H), 2.02–1.83 (m, 3H), 1.77–1.40 (m, 5H), 1.25–1.00 (m, 3H). MS (EI) for $C_{24}H_{27}Cl_4N_3O_2$, found 544.2 (MH⁺).

N-[(1S)-2-(3-Amino-8-azabicyclo[3.2.1]oct-8-yl)-1-[(2,4-dichlorophenyl)methyl]-2-oxoethyl]-1-(2,4-dichlorophenyl)cyclopropanecarboxamide (29). ¹H NMR (400 MHz, CD₃OD): δ 7.50–7.39 (m, 4H), 7.28–7.12 (m, 2H), 4.80–4.60 (m, 1H), 4.44–4.27 (m, 1H), 3.25–3.08 (m, 1H), 3.02–2.95 (m, 2H), 2.63–2.58 (m, 1H), 2.23–2.00 (m, 1H), 1.83–1.72 (m, 3H), 1.62–1.40 (m, 4H), 1.20–1.00 (m, 2H). MS (EI) for $C_{26}H_{27}Cl_4N_3O_2$, found 555.9 (M⁺).

N-[(1S)-2-(3-Amino-8-azabicyclo[3.2.1]oct-8-yl)-1-[(2,4-dichlorophenyl)methyl]-2-oxoethyl]-1-[4-[(trifluoromethyl)oxy]phenyl]cyclopropanecarboxamide (30). ¹H NMR (400 MHz, DMSO-*d*₆): δ 7.54 (m, 1H), 7.35 (m, 5H), 7.23 (m, 1H), 7.04 (m, 1H), 4.79 (m, 1H), 4.28 (m, 2H), 3.12–2.94 (m, 1H), 2.87 (m, 2H), 2.12–1.87 (m, 3H), 1.88–1.70 (m, 1H), 1.60 (m, 2H), 1.47 (m, 2H), 1.30–1.09 (m, 2H), 0.94 (m, 2H). MS (EI) for $C_{27}H_{28}Cl_2F_3N_3O_3$, found 571.4 (MH⁺).

N-[(1S)-2-(3-Amino-8-azabicyclo[3.2.1]oct-8-yl)-1-[(4-bromophenyl)methyl]-2-oxoethyl]-1-(2,4-dichlorophenyl)cyclopropanecarboxamide (31). ¹H NMR (400 MHz, CD₃OD): δ 8.57 (s, 1H), 7.50–7.38 (m, 3H), 7.15–7.00 (m, 3H), 4.84–4.80 (m, 1H), 3.63–3.43 (m, 2H), 4.18 (m, 1H), 3.23–3.18 (m, 1H), 3.19–2.99 (m, 2H), 2.83–2.78 (m, 3H), 2.58–2.50 (m, 1H), 2.39–2.30 (m, 1H), 2.16–2.03 (m, 1H), 1.98–1.80 (m, 1H), 1.60–1.40 (m, 5H), 1.20–1.05 (m, 2H). MS (EI) for $C_{26}H_{28}BrCl_2N_3O_2$, found 565.0 (MH⁺).

Biochemical Assay. The primary biochemical assay was a coupled experiment in which GCS activity was measured as the amount of UDP-glucose consumed during the synthase-catalyzed reaction. Upon quenching, remaining UDP-glucose was processed by UDP-glucose dehydrogenase, generating NADH. The NADH in turn participated in the diaphorase mediated reduction of resazurin to fluorescent resorufin. The more UDP-glucose remaining at the end of the reaction (i.e., the better the inhibitor), the more fluorescence was measured. Reactions were conducted in 384-well black, medium binding microtiter plates (Greiner). Synthase reaction mixtures

(25 mM HEPES, pH 7.4, 50 mM KCl and 5 mM MgCl₂) were prepared by first adding 0.0005 mL of compound in 100% DMSO to the plate. A volume $V = 0.010$ mL of 30 mol % C6-ceramide (Avanti Polar Lipids, Inc.) and 70 mol % dioleoylphosphatidylcholine (DOPC, Avanti Polar Lipids) with total concentration of 0.3 mM in 25 mM HEPES, pH 7.4, was added to the wells.²³ Full-activity controls (100% activity) contained DMSO only. No-activity control reactions (0% control) contained 0.010 mL of 100 mol % DOPC (0.3 mM) and DMSO only. The reactions were initiated by the addition of $V = 0.020$ mL of 0.020 mM UDP-glucose, 1.5 mg/mL CHAPS, 0.17 mg/mL GCS in 25 mM HEPES, pH 7.4, 75 mM KCl, and 7.5 mM MgCl₂ to all wells of the plate. The plate was kept at 26 °C for 3 h. The UDP-glucose that remains was measured by the addition of 0.015 mL of 0.30 mM NAD⁺, 0.30 mM resazurin, 0.11 mg/mL UDP-glucose dehydrogenase and 0.030 mg/mL diaphorase in 25 mM HEPES, pH 7.4, 50 mM KCl, and 5 mM MgCl₂. The plate was kept at 26 °C for 30 min or longer, and the increase in fluorescence with excitation at 530 nm and emission at 560 nm was measured with an Envision 1 plate reader (Perkin-Elmer). Consumption of UDP-glucose was limited to 40–60% of the total UDP-glucose in the assay.

IC₅₀ values were calculated by nonlinear regression analysis using the four-parameter equation $[Y = \max - (\max - \min)/(1 + (X/IC_{50})^N)]$ where Y is the observed fluorescence, X is the concentration of inhibitor, \max is the fluorescence in the absence of C6-ceramide (0% control), \min is the fluorescence in the absence of inhibitor (100% control), IC₅₀ is the concentration of inhibitor that gave 50% increase in fluorescence, and N is the empirical Hill slope. N should approximate unity. Curve fitting was performed using commercial software (IDBS ActivityBase XE).

Cellular Assay. The principal cellular readout used was the quantitation of ganglioside GM1 on the surface of A549 cells. Decreased glucosylceramide synthesis would lead to decreased GM1 synthesis. A549 cells were seeded in a 96-well plate at a density of 1000 cells/well in complete medium for 24 h at 37 °C. The cells were then treated with compounds for 72 h in the presence of 10% serum. On day 3, the cells were stained for 30 min at 4 °C with a fluorescent cholera toxin subunit B (FL-CTB) that binds to the ganglioside GM1 on the plasma membrane. The cells were then fixed with 3.7% formaldehyde prior to the addition of Hoechst stain. The plate was then read on an automated fluorescent microscope (ArrayScan from Cellomics) using a detection software algorithm (Spot Detector) to quantify the amount of gangliosides on the plasma membrane. The total intensity from the binding of FL-CTB to the membrane was normalized to the amount of cells in each well.

Microsomal Stability Assay. Microsomal oxidation of compounds was performed in the presence of mouse liver microsomes. In 96-well microtiter plates were added test compound (15 μM), microsomal protein (0.5 mg/mL), 1 mM NADPH in 100 mM potassium phosphate, pH 7.4 buffer, and 0.15% DMSO to a total volume of 100 μL/well. The mixtures were incubated at 37 °C for 30 min before being terminated by the addition of 50 μL of acetonitrile containing 20% acetic acid. Test compound concentrations were measured by LC/MS/MS and compared to no-NADPH control reactions to measure the extent of metabolism.

CYP Inhibition Assay. This assay was performed using pooled human liver microsomes and a cocktail of CYP substrates.²⁴ Compounds were incubated for 45 min with human liver microsomes (0.25 mg/mL) in the presence of NADPH (1 mmol) and substrates (20 μM). Changes in testosterone metabolism were used to measure compound inhibition of CYP3A4.

PD Experiment. C57Bl/6 mice were purchased from Taconic. Sprague–Dawley rats were purchased from Charles River Laboratories. The animals were fed normal chow (Purina 5001 or Purina 5010). Animals were dosed q.d. by oral gavage with study compound or vehicle. At the end of study, the animals were sacrificed by exsanguination. Liver and blood were collected for sphingolipid and glycosphingolipid analysis. The analysis was performed in a manner similar to what has been reported.²⁵

Rodent Efficacy Experiments. C57Bl/6 mice (Taconic) spent a total of 8 weeks on a high fat diet (Research Diets, D12492) before

being separated into dose groups by body weight ($n = 4$ animals/group). Six-week-old ZDF rats (Charles River) were fed a high fat diet (Purina 5008) and separated into groups of 8. The animals had ad libitum access to food and water except for the ZDF animals in the pair-fed study. In that study, two control groups were pair-fed to match ad libitum fed 32 or vehicle treated groups. On dose days 14 and 28, the animals were fasted for 5 h prior to bolus oral administration of glucose (2 g/kg), which was followed by a glucose tolerance test (0–120 min after glucose). At the end of the studies, animals were again fasted for 5 h prior to euthanasia. In the DIO studies, the mice were dosed with insulin before sacrifice in order to measure IR function. Plasma, liver, muscle, and white adipose tissue (WAT) were prepared and collected for PK, glycosphingolipid, insulin, glucose, and triglyceride analysis. Liver samples were also prepared for histopathology.

AUTHOR INFORMATION

Corresponding Author

*Phone: +1-650-837-7018. Fax: +1-650-837-8177. E-mail: sjr.researcher@gmail.com.

Author Contributions

[†]These authors contributed equally to this work.

Notes

The authors declare no competing financial interest.

ACKNOWLEDGMENTS

The authors are grateful to Sean Wu, Jing Wang, Eric Brooks, Lory Tan, and John Bui for collecting the reported ADME data. We also acknowledge our colleagues in the compound repository, Eliana Bustamante, Dorothy Trent, Melanie Dimapasoc, Yelena Zhrebina, Shaun Nguyen, and Josh Rulloda, for their support of this project. Thanks are extended to Chip Blazey, Jason Harris, and Henry Johnson for their review of this manuscript. Finally, we thank Tom von Geldern and Keith Woerpel for their guidance during many helpful discussions.

ABBREVIATIONS USED

GCS, glucosylceramide synthase; Cer, ceramide; GluCer, glucosylceramide; LacCer, lactosylceramide; GM3, ganglioside containing glucose, lactose, and sialic acid moieties; DIO, diet induced obese; ZDF, Zucker diabetic fatty; mpk, milligram of compound per kilogram of animal body weight; IR, insulin receptor; HbA1c, a measure of glycated hemoglobin; CYP3A4, cytochrome P450 isoform 3A4; WAT, white adipose tissue; TG, triglyceride; OGTT, oral glucose tolerance test; IGTT, intraperitoneal glucose tolerance test; SRT, substrate reduction therapy; ERT, enzyme replacement therapy; HATU, O-(7-azabenzotriazol-1-yl)-N,N',N'-tetramethyluronium hexafluorophosphate

REFERENCES

- (1) National Diabetes Fact Sheet, 2011. http://www.cdc.gov/diabetes/pubs/pdf/ndfs_2011.pdf (accessed December 2011).
- (2) Jonas, D.; Van Scoyoc, E.; Gerrald, K.; Wines, R.; Amick, H.; Runge, T.; Triplette, M. Drug Class Review: Newer Diabetes Medications, TZDs, and Combinations. <http://derp.ohsu.edu/about/final-document-display.cfm>, 2011.
- (3) (a) de Fost, M.; Aerts, J.; Hollak, C. Gaucher disease: from fundamental research to effective therapeutic interventions. *J. Med.* **2003**, *61*, 3–8. (b) Butters, T.; Mellor, H.; Narita, K.; Dwek, R.; Platt, F. Substrate reduction therapy in mouse models of the glycosphingolipidoses. *Philos. Trans. R. Soc. London, Ser. B* **2003**, *358*, 927–945.
- (4) Giraldo, P.; Alfonso, P.; Atutxa, K.; Fernández-Galán, M.; Barez, A.; Franco, R.; Alonso, D.; Martin, A.; Latre, P.; Poci, M. Real-world clinical experience with long-term miglustat maintenance therapy in

type 1 Gaucher disease: the ZAGAL project. *Haematologica* **2009**, *94*, 1771–1775.

(5) (a) Peterschmitt, M.; Burke, A.; Blankstein, L.; Smith, S.; Puga, A.; Kramer, W.; Harris, J.; Mathews, D.; Bonate, P. Safety, tolerability, and pharmacokinetics of eliglustat tartrate (Genz-112638) after single doses, multiple doses, and food in healthy volunteers. *J. Clin. Pharmacol.* **2011**, *51*, 695–705. (b) Lukina, E.; Watman, N.; Arreguin, E.; Banikazemi, M.; Dragosky, M.; Iastrebner, M.; Rosenbaum, H.; Phillips, M.; Pastores, G.; Rosenthal, D.; Kaper, M.; Singh, T.; Puga, A.; Bonate, P.; Peterschmitt, M. A phase 2 study of eliglustat tartrate (Genz-112638), an oral substrate reduction therapy for Gaucher disease type 1. *Blood* **2010**, *116*, 893–899.

(6) Yamashita, T.; Hashiramoto, A.; Haluzik, M.; Mizukami, H.; Beck, S.; Norton, A.; Kono, M.; Tsuji, S.; Daniotti, J.; Werth, N.; Sandhoff, R.; Sandhoff, K. Enhanced insulin sensitivity in mice lacking ganglioside GM3. *Proc. Natl. Acad. Sci. U.S.A.* **2003**, *100*, 3445–3449.

(7) (a) Tagami, S.; Inokuchi, J.; Kabayama, K.; Yoshimura, H.; Kitamura, F.; Uemura, S.; Ogawa, C.; Ishii, A.; Saito, M.; Ohtsuka, Y.; Sakaue, S.; Igarashi, Y. Ganglioside GM3 participates in the pathological conditions of insulin resistance. *J. Biol. Chem.* **2002**, *277*, 3085–3092. (b) Wennekes, T.; van den Berg, R.; Boot, R.; van der Marel, G.; Overkleeft, H.; Aerts, J. Glycosphingolipids: nature, function, and pharmacological modulation. *Angew. Chem., Int. Ed.* **2009**, *48*, 8848–8869.

(8) (a) Biochemical and cell data reported here were obtained in-house according to the text. The compounds tested were purchased or prepared at Exelixis or partner CRO. (b) Hirth, B.; Siegel, C. Synthesis of UDP-Glucose: N-Acylsphingosine Glucosyltransferase Inhibitors. U.S. Patent 6,855,830 B2, February, 15, 2005; Genzyme Co., U.S.

(9) Aerts, J.; Ottenhoff, R.; Powlson, A.; Grefhorst, A.; van Eijk, M.; Dubbelhuis, P.; Aten, J.; Kuipers, F.; Serlie, M.; Wennekes, T.; Sethi, J.; O'Rahilly, S.; Overkleeft, H. Pharmacological inhibition of glucosylceramide synthase enhances insulin sensitivity. *Diabetes* **2007**, *56*, 1341–1349.

(10) Bijl, N.; Sokolović, M.; Vrans, C.; Langeveld, M.; Moerland, P.; Ottenhoff, R.; van Roomen, C.; Claessen, N.; Boot, R.; Aten, J.; Groen, A.; Aerts, J.; Eijk, M. Modulation of glycosphingolipid metabolism significantly improves hepatic insulin sensitivity and reverses hepatic steatosis in mice. *Hepatology* **2009**, *50*, 1431–1441.

(11) Wennekes, T.; Meijer, A.; Groen, A.; Boot, R.; Groener, J.; van Eijk, M.; Ottenhoff, R.; Bijl, N.; Ghauharali, K.; Song, H.; O'Shea, T.; Liu, H.; Yew, N.; Copeland, D.; van den Berg, R.; van der Marel, G.; Overkleeft, H.; Aerts, J. Dual-action lipophilic iminosugar improves glycemic control in obese rodents by reduction of visceral glycosphingolipids and buffering of carbohydrate assimilation. *J. Med. Chem.* **2010**, *53*, 689–698.

(12) Zhao, H.; Przybylska, M.; Wu, I.; Zhang, J.; Siegel, C.; Komarnitsky, S.; Yew, N.; Cheng, S. Inhibiting glycosphingolipid synthesis improves glycemic control and insulin sensitivity in animal models of type 2 diabetes. *Diabetes* **2007**, *56*, 1210–1218.

(13) Zhao, H.; Przybylska, M.; Wu, I.; Zhang, J.; Maniatis, P.; Pacheco, J.; Piepenhagen, P.; Copeland, D.; Arbeen, C.; Shayman, J.; Aerts, J.; Jiang, C.; Cheng, S.; Yew, N. Inhibiting glycosphingolipid synthesis ameliorates hepatic steatosis in obese mice. *Hepatology* **2009**, *50*, 85–93.

(14) Yew, N.; Zhao, H.; Hong, E.; Wu, I.; Przybylska, M.; Siegel, C.; Shayman, J.; Arbeen, C.; Kim, J.; Jiang, C.; Cheng, S. Increased hepatic insulin action in diet-induced obese mice following inhibition of glucosylceramide synthase. *PLoS One* **2010**, *5*, e11239.

(15) Koltun, E.; Richards, S.; Chan, V.; Nachtigall, J.; Du, H.; Noson, K.; Galan, A.; Aay, N.; Hanel, A.; Harrison, A.; Zhang, J.; Won, K.; Tam, D.; Qian, F.; Wang, T.; Finn, P.; Ogilvie, K.; Rosen, J.; Mohan, R.; Larson, C.; Lamb, P.; Nuss, J.; Kearney, P. Discovery of a new class of glucosylceramide synthase inhibitors. *Bioorg. Med. Chem. Lett.* **2011**, *21*, 6773–6777.

(16) Aay, N.; Aoyama, R.; Arcalas, A.; Chan, V.; Du, H.; Kearney, P.; Koltun, E.; Nachtigall, J.; Pack, M.; Richards, S. Inhibitors of Glucosylceramide Synthase. WO 2010/091164 A1, 2010.

(17) Doses of 7 and 6 were chosen based on reported efficacious doses in refs 10 and 13.

(18) Barrie, C.; Cantello, M.; Cawthorne, M.; Cottam, G.; Duff, P.; Haigh, D.; Hindley, R.; Lister, C.; Smith, S.; Thurlby, P. [[ω -(Heterocyclylamino)alkoxy]benzyl]-2,4-thiazolidinediones as potent antihyperglycemic agents. *J. Med. Chem.* **1994**, *37*, 3977–3985.

(19) Garofalo, R.; Orena, S.; Rafidi, K.; Torchia, A.; Stock, J.; Hildebrandt, A.; Coskran, T.; Black, S.; Brees, D.; Wicks, J.; McNeish, J.; Coleman, K. Severe diabetes, age-dependant loss of adipose tissue, and mild growth deficiency in mice lacking Akt2/PKB β . *J. Clin. Invest.* **2003**, *112*, 197–208.

(20) (a) Chen, D.; Liao, J.; Li, N.; Zhou, C.; Liu, Q.; Wang, G.; Zhang, R.; Zhang, S.; Lin, L.; Chen, K.; Xie, X.; Nan, F.; Young, A.; Wang, M. A nonpeptidic agonist of glucagon-like peptide 1 receptors with efficacy in diabetic *db/db* mice. *Proc. Nat. Acad. Sci. U.S.A.* **2007**, *104*, 943–948. (b) Gredulin, B.; Smith, P.; Prickett, K.; Tryon, M.; Barnhill, S.; Reynolds, J.; Nielsen, L.; Parkes, D.; Young, A. Dose-response for glycaemic and metabolic changes 28 days after single injection of long-acting release exenatide in diabetic Zucker rats. *Diabetologia* **2005**, *48*, 1380–1385.

(21) Cable, E.; Finn, P.; Stebbins, J.; Hou, J.; Ito, B.; van Poelje, P.; Linemeyer, D.; Erion, M. Reduction of hepatic steatosis in rats and mice after treatment with a liver-targeted thyroid hormone receptor agonist. *Hepatology* **2009**, *49*, 407–417.

(22) Manuel, M.; Teletin, M.; Antal, C.; Wendling, O.; Auwerx, J.; Heikkinen, S.; Khetchoumian, K.; Argmann, C.; Dgheem, M. Histopathology in mouse metabolic investigations. *Curr. Protoc. Mol. Biol.* **2007**, 29B.4.1–29B.4.32.

(23) ¹C6-ceramide and DOPC are prepared as 20 mg/mL stock solutions in 95% ethanol and stored at –20 °C. The appropriate volumes are transferred to a 40 mL glass vial with screw-cap septum and taken to dryness with a stream of argon gas. The lipids are resuspended in 1 mL of distilled H₂O, frozen, and lyophilized overnight. The lipids are hydrated by first adding enough 25 mM HEPES, pH 7.4, to give 4× the required concentration for addition to the plate, vortexing to suspend the lyophilized lipids, and waiting for 1 h or more. The solution is then frozen, placed in a bath sonicator, and thawed with sonication. This is repeated three additional times to give four freeze–thaw sonication cycles. The resulting solution is diluted 4-fold with 25 mM HEPES, pH 7.4, to give the solution of lipids that is added to the plate.

(24) Tolonen, A.; Petsalo, A.; Turpeinen, M.; Uusitalo, J.; Pelkonen, O. In vitro interaction cocktail assay for nine major cytochrome P450 enzymes with 13 probe reactions and a single LC/MSMS run: analytical validation and testing with monoclonal anti-CYP antibodies. *J. Mass Spectrom.* **2007**, *42*, 960–966.

(25) Groener, J.; Poorthuis, B.; Kuiper, S.; Helmond, M.; Hollak, C.; Aerts, J. HPLC for simultaneous quantification of total ceramide, glucosylceramide, and ceramide trihexoside concentrations in plasma. *Clin. Chem.* **2007**, *53*, 742–747.